

January 2016

Restoring Consciousness During Seizures With Deep Brain Stimulation

Adam Joseph Kundishora
Yale University, adam.kundishora@gmail.com

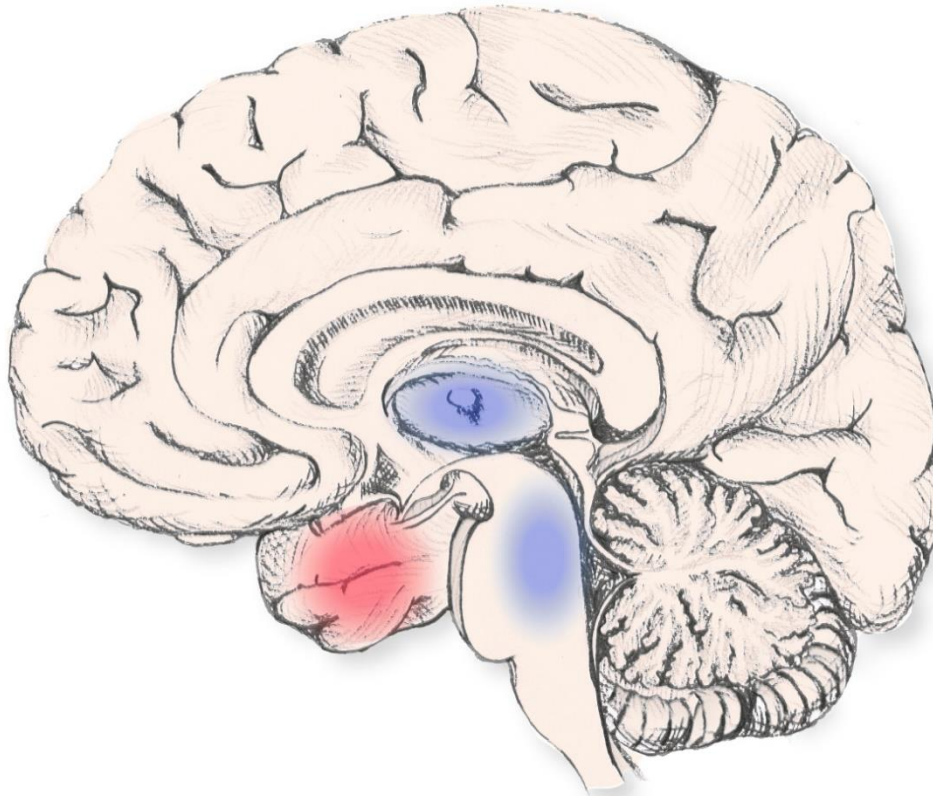
Follow this and additional works at: <http://elischolar.library.yale.edu/ymtdl>

Recommended Citation

Kundishora, Adam Joseph, "Restoring Consciousness During Seizures With Deep Brain Stimulation" (2016). *Yale Medicine Thesis Digital Library*. 2063.
<http://elischolar.library.yale.edu/ymtdl/2063>

This Open Access Thesis is brought to you for free and open access by the School of Medicine at EliScholar – A Digital Platform for Scholarly Publishing at Yale. It has been accepted for inclusion in Yale Medicine Thesis Digital Library by an authorized administrator of EliScholar – A Digital Platform for Scholarly Publishing at Yale. For more information, please contact elischolar@yale.edu.

Restoring consciousness during seizures with deep brain stimulation



A Thesis Submitted to the
Yale University School of Medicine
in Partial Fulfilment of the Requirements for the
Degree of Doctor of Medicine

By
Adam Joseph Kundishora
2016

Dedication

To:

My dearest wife, Abbie
Whose patience and support
Knows no bounds

and

My sister, Karyn
Whose life was cut too short
Just one year prior to this work
Because of seizures

Abstract

Impaired consciousness occurs suddenly and unpredictably in people with epilepsy, markedly worsening quality of life and increasing risk of mortality. Focal seizures with impaired consciousness are the most common form of epilepsy, and are refractory to all current medical and surgical therapies in about one sixth of cases. Restoring consciousness during and following seizures would be potentially transformative for these individuals. Here, we investigate deep brain stimulation to improve level of conscious arousal in a rat model of focal limbic seizures. We found that dual-site stimulation of the thalamic intralaminar central lateral nucleus (CL) and pontine nucleus oralis (PnO) bilaterally during focal limbic seizures restored normal-appearing cortical electrophysiology and markedly improved behavioral arousal. In contrast, single-site bilateral stimulation of CL or PnO alone was insufficient to achieve the same result. These findings support the 'network inhibition hypothesis' that focal limbic seizures impair consciousness through widespread inhibition of subcortical arousal. Driving subcortical arousal function would be a novel therapeutic approach to some forms of refractory epilepsy and may be compatible with devices already in use for responsive neurostimulation. Multi-site deep brain stimulation of subcortical arousal structures may benefit not only patients with epilepsy, but also other disorders of consciousness.

Table of Contents

Title Page	1
Dedication	2
Abstract	3
Statement of purpose	6
Introduction	6
Methods	8
Animals	8
Surgery and electrode implantation	8
Electrophysiology and video recording procedures	11
Histology	15
Data analysis and statistics	16
Statement of labor	18
Results	19
Cortical physiological arousal with PnO stimulation under deep anesthesia	19
Cortical physiological arousal with PnO stimulation during focal limbic seizures	20
Cortical physiological arousal with PnO stimulation during focal limbic seizures in awake animals led to minimal improvement in behavior	22
Dual-site CL and PnO stimulation improves cortical physiological arousal during focal limbic seizures	23
Dual-site CL and PnO stimulation markedly improves behavioral arousal during focal limbic seizures	24
Discussion	26
Acknowledgements	32
References	33
Figures	37
Figure 1	37
Figure 2	39
Figure 3	40
Figure 4	41

Figure 5	43
Figure 6	44
Figure 7	45
Supplementary Figure 1.....	46
Supplementary Figure 2.....	48
Supplementary Figure 3.....	49
Supplementary Figure 4.....	51
Video Supplement	52
Appendix A, Additional information on stimulus parameters	53
Appendix B, Additional information on other arousal nuclei	54
Cortical physiological arousal with CM stimulation under deep anesthesia and during limbic seizure	54
Cortical physiological arousal with Vm stimulation under deep anesthesia and during limbic seizure	55
Cortical physiological arousal with DpMe stimulation under deep anesthesia and during limbic seizure	55
Appendix Figures	57
Appendix Figure 1	57
Appendix Figure 2	58
Appendix Figure 3	59
Appendix Figure 4	61

Statement of purpose

We aimed to demonstrate a proof-of-principle improvement in electrophysiological and behavioral measures of consciousness during seizures with contemporaneous stimulation of multiple arousal nuclei. We hypothesized that electrically stimulating some combination of one or more known arousal nuclei would lead to mitigation or complete reversal of the loss of consciousness associated with focal limbic seizures.

Introduction

Impaired consciousness associated with refractory seizures severely impacts the productivity, safety, and quality of life of patients suffering from epilepsy (1-3). In addition, impaired consciousness during seizures is associated with a crippling social stigma that is only mitigated by complete seizure control, something that is out of reach for nearly a quarter of all patients with epilepsy. Neurostimulation has grown in recent years as a treatment for refractory epilepsy, but still leaves many patients without complete seizure freedom (4-6). For these patients, a strategy aimed at improving quality of life, morbidity, and mortality despite ongoing seizures could be highly beneficial.

Consciousness depends on several functions including: 1. specific sensorimotor and other systems constituting the content of consciousness; and 2. systems regulating the overall level of consciousness manifested as awareness, attention, and basic conscious arousal(3, 7-11).

Importantly conscious arousal, which distinguishes coma or deep sleep from the alert state, can be assessed by relatively simple behavioral and physiological observations and forms the crucial

necessary first step enabling other higher-order aspects of consciousness to occur(9). The mechanism by which consciousness is lost during and after temporal lobe, focal limbic seizures has been explored and consolidated in the “network inhibition hypothesis”(3, 12) (Fig. 1 A). Recent animal studies (13-17) and human data (18-21) point to functional de-afferentation of the cortex as central to the loss of consciousness (10, 22). Inhibition of subcortical arousal structures including the upper brainstem reticular formation and one of its direct targets, the intralaminar thalamus during seizures, may result in cortical states resembling deep sleep or coma (3) (Fig. 1 A). The effect on subcortical arousal structures themselves are characterized by decreased ictal firing rate and decreased cholinergic release from intralaminar thalamic neurons, decreased fMRI BOLD signal from the intralaminar thalamic region, and decreased ictal firing rate of serotonergic medullary raphe neurons, among others(14, 23). Thus, therapeutic activation of these subcortical arousal structures could attenuate the loss of consciousness experienced in focal limbic seizures (Fig. 1 B).

Previous studies investigating the intralaminar thalamus and pontine reticular formation provide a basis for further exploration. The general role of intralaminar thalamus in attention, arousal, and consciousness, has been repeatedly described over many years (24-28). More recently, electrical stimulation of this region in animal models and humans has yielded promising results regarding its capacity to improve arousal during pathologic states of decreased consciousness (13, 29). Likewise, early stimulation studies in the upper brainstem reticular formation also showed electrophysiological wake-like cortical activity in animals under anesthesia (30, 31). However, the use of electrical stimulation of these subcortical arousal

regions to maintain or improve consciousness during a seizure has not previously been described.

Relative to more common applications of therapeutic neurostimulation for movement disorders or aborting/preventing seizures, targets and methods for promoting consciousness are poorly developed (32). Therefore, we propose a new strategy for addressing the loss of consciousness in focal limbic seizures based on the current proof-of-principle pre-clinical study. We electrically stimulated both the central lateral nucleus of the intralaminar thalamus (CL) and the pontine nucleus oralis (PnO, a member of the pontine reticular formation) in anesthetized and awake behaving animals during focal limbic seizures. By assessing electrophysiological and behavioral metrics of consciousness, we provide evidence that deep brain stimulation can reduce cortical slow-wave activity, increase multi-unit cortical activity, and increase behavioral arousal *during seizures*.

Methods

Animals

The Yale University Institutional Animal Care and Use Committee approved all procedures. Adult female Sprague-Dawley rats weighing 200-280 grams (Charles River Laboratories) were used.

Surgery and electrode implantation

The animal model of focal limbic seizures was prepared as described previously (15) with the modifications described below. Animals were deeply anesthetized with an intramuscular injection of 80-90 mg/kg ketamine (Henry Schein Animal Health, Ashburn, VA, U.S.A.) and 15 mg/kg xylazine (AnaSed; Lloyd Laboratories, Quezon City, Philippines). Craniotomies were placed stereotactically over sites of planned electrode placement, as well as for 4-5 stainless steel anchoring screws (0-80 x 3/32; PlasticsOne, Roanoke, VA, U.S.A.) and a ground screw (E363-20; PlasticsOne) (Supp. 1 A).

To monitor changes in cortical physiology with focal limbic seizures and deep brain stimulation we chose to record from lateral orbital frontal cortex (LOFC). This region demonstrates typical ictal and postictal slow wave activity as well as changes in functional neuroimaging, which are also present in other widespread cortical regions in both animal models and human studies(13-16, 18, 19).

All coordinates are reported as final electrode tip locations in reference to bregma(33). For 'acute preparations', a single tungsten monopolar micro-electrode (UEWMGGSEDNNM; FHC, Bowdoin, ME, U.S.A.) with an impedance of 2-4 M Ω was implanted at an approach angle of 20 degrees from vertical to record local field potentials in the right lateral orbitofrontal cortex (LOFC); anterior-posterior (AP) +4.2 mm, medial-lateral (ML) -2.2 mm, superior-inferior (SI) -4.2 mm (33). In order to overcome the stimulation artifact that obscures multi-unit data, a second differential recording electrode was custom modified by affixing two tungsten monopolar electrodes (UEWMGGSEDNNM; FHC) with impedances of 3-4 M Ω together with bonding

cement (Krazy glue, Elmer's Products, Inc. Westerville, OH) such that their tips were separated by less than 0.5 mm and it was implanted at an approach angle of 20 degrees from vertical in the left lateral orbitofrontal cortex; AP +4.2, ML +2.2, SI -4.2 mm. This unique configuration of two high impedance electrodes in close proximity had the effect of subtracting out the large shared noise signal while preserving the independent neuronal signals close to each electrode tip. For 'chronic preparations', a stainless-steel twisted-pair bipolar electrode (E363-2-2TW; PlasticsOne) cut to 20 mm and with electrode tips separated by 1 mm in the coronal plane was implanted at an angle of 20 degrees into the right lateral orbitofrontal cortex (AP +4.2, ML -2.2, SI -4.2 mm). Hippocampal electrodes were bilaterally implanted for acute preparations in order to mitigate hippocampal fatigue whereas in chronic preparations a unilateral electrode was placed, secondary to space limitations. Twisted pair bipolar electrodes with tips separated by 1 mm, insulation shaved to 0.5 mm, and electrode tips in the coronal plane were implanted into the dorsal hippocampus (HC) (AP -3.8, ML \pm 3.4, SI -3.6 mm). For acute and chronic preparations involving the central lateral intralaminar thalamus (CL), two twisted-pair bipolar electrodes with electrode tips in the sagittal plane were implanted in bilateral CL (AP -2.8; ML \pm 1.4; SI -5.2 mm). For acute and chronic preparations involving the pontine nucleus oralis (PnO), two twisted-pair bipolar electrodes with electrode tips in the sagittal plane were implanted at an approach angle of 20 degrees in bilateral PnO (AP -8.0; ML \pm 1.4; SI -8.0 mm).

In chronic experiments, electrodes were firmly cemented to nearby anchoring screws with dental cement (Lang Dental Manufacturing, Wheeling, IL, U.S.A.). All electrode pins except for the ground pin were carefully bent and placed into two, 6-pin pedestals (MS363; PlasticsOne).

The ground pin was bonded to the outside of the caudal-most pedestal (Krazy glue, Elmer's Products, Inc.) and the whole assembly was sealed with silicon sealant for insulation (Kwik-cast, World Precision Instruments, Inc. Sarasota, FL, U.S.A.). Skin was reapproximated with interrupted silk sutures (Surgical Specialties Corp., Vancouver, BC, Canada) around each pedestal. Chronic recordings began at least 48 hours postoperatively.

In a set of different animals, additional implantations in the central medial (CM), ventromedial (Vm), and deep mesencephalic (DpMe) nuclei were performed during an exploratory phase in which multiple known arousal nuclei were tested for effect of stimulation under anesthesia and seizure (see Appendix B).

Electrophysiology and video recording procedures

We performed electrophysiological recordings under the following conditions: (1) Acute experiments under deep anesthesia were performed with ketamine/xylazine 80-90/15 mg/kg anesthesia, injected intramuscularly, resulting in the presence of continuous cortical slow waves during which no seizures were triggered; (2) acute experiments under light anesthesia were done after animals had recovered from deep anesthesia to a state whereby slow waves occurred at approximately <3 waves per 10 s of recordings as described previously (15); (3) experiments in chronically implanted, behaving animals were performed in the awake state, under deep anesthesia, under anesthesia-induced sleep with a low dose of intramuscular-injected ketamine/xylazine 15/3 mg/kg, or during naturally occurring sleep.

Stimulations of CL and/or PnO were generated by independent isolated pulse stimulators (Model 2100, A-M systems, Sequim, WA, U.S.A.). For all experiments, CL and PnO stimulus parameters were titrated per animal in the acute setting under deep anesthesia, unilaterally on each side to determine effective stimulus parameters to produce physiologic cortical arousal. Stimulations in acute animals under deep anesthesia and in chronically implanted animals under anesthesia or during sleep were 20 s duration. Stimulations during focal limbic seizures were 120 s. This duration was chosen to include the majority of the seizure in most cases (mean seizure duration = 57.9 ± 8.4 s) and often included part of the postictal period. Stimulus frequencies were chosen based on prior work (13) and pilot experiments (not shown) demonstrating that a frequency of approximately 100 Hz was most effective in CL and approximately 50 Hz in PnO to produce cortical physiological arousal. Stimulus current amplitudes were then titrated individually per animal. CL was initially stimulated with a square biphasic pulse (0.5 ms/phase) at 100 Hz (13) in a range from 150 – 400 μ A per side during titration. The eventual acute experimental amplitudes of stimulation fell between 150 – 400 μ A split bilaterally (approximately 75 – 200 μ A per side); the higher amperages during titration were tested to ensure a lack of afterdischarges or seizure induction from the stimulation. PnO was stimulated in acute experiments with a square biphasic pulse (0.5 ms/phase) at 50 Hz and titration was in the same fashion as CL (range 35 – 200 μ A unilaterally, or 70 – 400 μ A split bilaterally). Sham stimulation of CL and PnO was performed with 0.2 μ A split bilaterally.

For chronic experiments, a secondary titration was performed at least 48 hr post-operatively to account for any change in electrode impedance secondary to gliosis at the intraparenchymal

electrode tip. Stimulus titration was again performed under deep anesthesia without seizures. Final ranges of stimulation delivered bilaterally in all experiments were as follows: acute PnO only 70 – 400 μ A; acute CL only 400 μ A; chronic PnO only 70 – 400 μ A; dual site CL: 150 – 350 μ A, PnO 50 – 300 μ A. For these stimuli delivered bilaterally the current reaching each side was approximately 50 % of the total.

Focal limbic seizures in acute and chronic experiments were induced with a two-second biphasic square pulse at 60 Hz in the unilateral hippocampus (1 ms/phase) generated by a WPI linear stimulus isolator (Model A395, World Precision Instruments, Inc.) with current ranging from 100 μ A to 1.5 mA, adjusted to obtain focal hippocampal seizures of at least 15 s duration, without generalization of poly-spike discharges to LOFC. Stimulations were manually triggered by keyboard input via custom Spike2 (version 5.2, CED, Cambridge, U.K.) scripts running through a digital-to-analogue converter (Power 1401; CED). Seizures in acute experiments were induced from a state of light anesthesia as described previously (14, 15). Seizures in chronically implanted animals were induced in the awake state. In one animal seizures were induced 15 minutes after administration of 0.9 mg/kg diazepam IM to prevent seizure generalization as described previously (16).

CL and PnO stimulations done under low-dose anesthesia without seizures in chronically implanted animals were performed after intramuscular injection of approximately 15 mg/kg ketamine and 3 mg/kg xylazine. This dose was selected to attain sufficient anesthetic depth to produce a state of slow-wave activity and behavioral arrest without deepening anesthesia to

surgical depth. CL only, PnO only, and dual-site stimulation were also performed during periods of naturally occurring sleep. In all cases sham stimulations (0.2 μ A split bilaterally) of CL and PnO were alternated with true stimulations.

Recordings of cortical, HC, CL, and PnO signals were done on separate channels of microelectrode amplifiers (A-M systems Model 1800). In acute recordings from LOFC where high impedance FHC electrodes were used, local field potentials (LFP) were recorded via the monopolar electrode and multi-unit activity (MUA) was recorded via the custom-assembled differential recording electrode described above. MUA was recorded with 1000X amplifier gain and then high pass filtered at 400 – 10,000 Hz with an additional 2.0 dB gain using a digital filter (Model 3364; Krohn-Hite, Brocton, MA, U.S.A.). LFP signals for acute recordings were recorded with 1000X amplifier gain and filtered at 1 to 500 Hz. Cortical LFP were further low pass filtered at 100 Hz with an additional 1.5 dB gain using a digital filter (Model 3364; Krohn-Hite).

In chronically implanted animals, in which only bipolar LFP electrodes were used for recording and stimulation, two 6-pin connector wires (PlasticsOne) were connected to a single 12 pin commutator (PlasticOne). The commutator was then connected to the head stages of the A-M Systems amplifiers using 2 customized 6-pin connectors (363SL-6; PlasticsOne). The ground wire was connected separately to a common ground inside the Faraday cage, which in turn was connected to the building ground. HC, CL, PnO, and cortical signals were filtered at 1-500 Hz on the recording amplifiers with 1000X gain. Cortical LFP activity was then further filtered with a 50 Hz lowpass filter with an additional 1.5 dB gain via a digital filter (Model 3364; Krohn-Hite).

All signals in both acute and chronic experiments were digitized with an analog-to-digital converter (Power 1401; CED) using Spike2 (Version 5.2; CED). Cortical and HC LFP were sampled at 1000 Hz; cortical MUA was sampled at 20,000 Hz. For chronic recordings, electrophysiology-synchronized video was captured with a digital camera (Hercules, La Gacilly, France) and recorded with Spike2 Video Recorder (CED).

After completing all electrophysiological recordings, animals were sacrificed with a 0.5 mL intraperitoneal injection of pentobarbital sodium and phenytoin sodium solution (Euthasol; Virbac, Fort Worth, TX, U.S.A.) for histologic localization of electrodes.

Histology

Animals were perfused transcardially with 0.1 % heparinized phosphate-buffered saline (PBS) (APP Pharmaceuticals, Lake Zurich, IL, U.S.A.) followed by 4 % paraformaldehyde (JT Baker, Center Valley, PA, U.S.A.) in PBS. The brain was then removed and post-fixed for at least 48 hours in 4 % paraformaldehyde (PFA) in PBS at 4°C. Brains were washed three times in PBS in preparation for slicing, placed in 2 % agarose gel (American Bioanalytical, Natick, MA, U.S.A.) and cut at 100 µm on a Vibratome (Leica Microsystems, Wetzlar, Germany). Slices were mounted on polarized slides (ThermoScientific, Waltham, MA, U.S.A.) and dried for at least 72 hours. Slides were stained with cresyl violet using a manufacturer-recommended protocol for reagents (FD NeuroTechnologies, Columbia, MD, U.S.A.) in order to confirm electrode location. Slides were then cover-slipped with Permount (Fisher Chemicals, Pittsburg, PA, U.S.A.). Images of slices were taken at 40X magnification on a compound light microscope (Carl Zeiss,

Oberkochen, Germany), imaged with a digital camera (Motic, Hong Kong), and digitally stitched together (Microsoft Image Composite Editor, Redmond, WA, U.S.A.). Electrode locations for PnO were confirmed when they fell ventral to the superior cerebellar peduncle, lateral to the paramedian raphe nucleus, medial to the ventral nucleus of the lateral lemniscus, and dorsal to both the ventrolateral tegmental area and the reticulotegmental nucleus of the pons (Supp. 1 B). Electrode locations for CL were confirmed when they fell no more than 1.5 mm ventral to the hippocampus, in the dorsal thalamus, and were just lateral to the stria medullaris/lateral habenula complex or the mediodorsal thalamic nucleus (Supp. 1 C).

Data analysis and statistics

Data were analyzed in Spike2 (CED) and Microsoft Excel (Microsoft, Redmond, WA, U.S.A.).

Analysis epochs were defined as follows: During experiments under deep anesthesia, the Pre-DBS epoch was defined as the 20 s immediately prior to stimulation; intra-DBS was defined as the whole 20 s stimulation; post-DBS was defined as the 20 s immediately following stimulation. For timecourse analysis following DBS we also used 10 s epochs extending from 0 to 60 s after DBS. During all other experiments, the baseline epoch was defined as the 30 s immediately preceding hippocampal stimulation; ictal pre-DBS was defined as the time immediately following hippocampal stimulation to the time immediately preceding PnO or CL stimulation; ictal DBS was defined as the time during which DBS and seizure were occurring simultaneously; postictal DBS was defined as the time immediately following seizure, during DBS; postictal post-DBS was defined as the 30 s immediately following the termination of DBS.

Any seizures exhibiting secondary generalization based on poly-spike discharges in the frontal cortical LFP during the analysis epochs were excluded (34). For each epoch, cortical LFP power was determined by fast Fourier transform (bin size 1/1.024 Hz, non-windowed). In all trials, power was then normalized to the maximum power in the baseline epoch. Multi-unit data were first spike sorted in Spike2 (CED) using the template-matching method to identify up to 3 units per recording session. To distinguish periodic unit firing versus more continuous tonic firing, autocorrelograms were generated in Spike2 (see Fig. 4 B for examples) and further analyzed in Excel. Periodicity was quantified from the autocorrelograms by taking the average amplitudes (absolute value) of the first minimum (greatest anti-correlation) and first maximum (greatest correlation) moving away from time zero. During epochs where there was no periodic firing (typically the baseline and ictal DBS epochs, see Fig. 4 B), the maximum and minimum times of the ictal pre-DBS epoch from the same trial were applied to the other epochs for purposes of direct comparison. Average spike rate within each epoch was calculated using Spike2 (CED).

During trials in chronically implanted animals, behavioral level of arousal was measured using a modified version of a scale previously developed and used in this animal model (13, 16). A score of 0 – 4 was assigned for each epoch: 0 for no exploratory behavior with the animal lying on its side or lying asleep; 1 for being upright/lying awake with its ventral surface on the floor of the cage (righting reflex intact); 2 for forepaw exploratory movements on the floor of the cage or actively sniffing the floor of the cage; 3 for forepaws used to explore the sides of the cage; 4 for locomotion requiring movement of both forelimbs and hind limbs. The highest behavioral

score achieved in an epoch was assigned as the score for that epoch. Scoring of all epochs was performed by each of two observers, one of whom was blinded to epoch identity and stimulation (sham or true) conditions. Discrepancies of one point between observations were averaged. No discrepancies of more than one point were assigned during the scoring for any epoch, suggesting relatively good inter-observer reliability.

Between 2 and 9 focal limbic seizures or stimulations were obtained during experiments in each animal. In all analyses, intra-animal data were averaged before performing group analysis so that the sample size equaled the number of animals. This approach provides a more conservative estimate of sample size; however, similar results were obtained in all cases if group analyses were instead performed by total numbers of seizures or stimulations (data not shown). Data are reported as group mean \pm standard error of mean. Statistical significance was assessed by two-tailed Student's *t*-test with threshold $p = 0.05$ corrected for multiple comparisons using the Bonferroni-Holm method.

Statement of labor

All acute PnO, CM, Vm, and DpMe implantations were performed by Adam Kundishora. 3 acute implantations of CL only were performed by a fellow medical student. All chronic implantations of PnO and PnO + CL were performed by Adam Kundishora. All acute histology was performed by Adam Kundishora. 6 chronically implanted animals were histologically prepared by an undergraduate student, then analyzed photographically by Adam Kundishora. All data analysis, statistics, and figure generation was done by Adam Kundishora.

Results

Cortical physiological arousal with PnO stimulation under deep anesthesia

We electrically stimulated bilateral pontine nucleus oralis (PnO) in animals under deep anesthesia to determine stimulus parameters (see Methods) effective in producing physiological cortical arousal as measured by increased cortical desynchronization and increased cortical tonic spiking rates.

The large-amplitude 1-3 Hz slow waves that are prominent and continuous in the cortical LFP during deep anesthesia were eliminated during and after PnO DBS (Supp. 2). Persistent cortical desynchronization during and after the stimulus was associated with a sustained increase in neuronal activity as measured by cortical MUA (Supp. 2 B middle and right trace). No afterdischarges or seizure-like activity were measured in the PnO or hippocampal electrodes during or after stimulation with the current ranges used in our experiments.

To quantify loss of low-frequency cortical activity, LFP power (normalized to the maximum pre-stimulus power within animal) was measured in epochs immediately prior to, during, and after DBS. We observed decreases in low-frequency power during and after DBS, especially in the delta-band frequencies (Supp. 2 C; n= 7 animals; 4 animals excluded due to inaccurate electrode placement). This decrease persisted for over 60 s after stimulation (Supp. 2 D), and was not present with PnO sham DBS (Supp. 2 D; n= 7) or in animals in which the electrodes fell

outside the target area (data not shown; $n=4$). Average delta-band power (0-4 Hz) was significantly decreased ($-73.5 \pm 5.1\%$) during DBS compared to pre-DBS (Supp. 2 E; $n=7$; $p < 0.0001$, Bonferroni-Holm corrected). No significant change in delta-band power was measured with PnO sham DBS compared to the pre-DBS epoch (Supp. 2 E; $n=7$; $p=0.58$).

Cortical physiological arousal with PnO stimulation during focal limbic seizures

Animals that were initially anesthetized to surgical depth were allowed to recover to a level of light anesthesia indicated by a predominance of cortical fast activity on LFP as described previously (15, 16). Focal limbic seizures were then induced with a 2 s hippocampal stimulation. Approximately 10 s after seizure onset, during which time it was determined that there was no secondary generalization of the seizure, bilateral PnO were again stimulated at an amplitude between 70 and 400 μA , titrated per animal or 0.2 μA sham stimulation. During seizures, prior to PnO DBS, we observed cortical slow waves (Fig. 2 A, B), previously known to occur during and after focal limbic seizures (15, 16, 19). PnO DBS during the ictal and postictal states abolished cortical slow waves both during and after stimulation (Fig. 2 A, B). PnO DBS was also associated with persistently increased cortical activity during and after stimulation as indicated by sustained MUA increases and persistently desynchronized cortical activity as indicated by a shift from phasic to tonic firing states (Fig. 2 A, B).

Group analysis of cortical LFP showed decreases in low-frequency power during and after PnO stimulation both ictally and postictally (Fig. 3 A, B; $n=9$; 9 animals excluded due to inaccurate electrode placement). These changes appeared very similar to those seen under deep

anesthesia without seizures (Supp. 2 C). Delta-band power during the ictal DBS epoch was significantly decreased as compared to the ictal pre-DBS epoch ($-64.1 \pm 5.0 \%$) ($n=9$; $p < 0.001$, Bonferroni-Holm corrected) (Fig. 3 B, C). This was in contrast to the lack of a decrease seen with sham DBS ($n=7$; $p < 0.17$). Cortical delta band power during and after PnO DBS remained similar to baseline delta power, and significantly lower than sham stimulation delta-band power throughout all DBS and post-DBS time epochs (Fig. 3 B; $n=9$ for DBS; $n=7$ for sham controls; ictal DBS $p < 0.01$; postictal DBS $p < 0.02$; postictal post-DBS $p < 0.006$, Bonferroni-Holm corrected). In contrast, sham-DBS controls showed elevated cortical delta power throughout the ictal and postictal periods (Fig. 3 B) which appeared electrographically identical to the ictal pre-DBS epochs (Fig. 2). Although DBS significantly reduced cortical delta power, seizure duration, as defined by the hippocampal recording, was not significantly changed, lasting 72.2 ± 15.4 s with DBS and 83.6 ± 16.9 s for sham controls ($n=9, 7$ respectively; $p=0.64$).

In acute experiments under light anesthesia, we also investigated the effects of PnO stimulation on cortical neuronal firing to confirm that the observed LFP changes during focal limbic seizures indeed represented increased cortical arousal. During seizures, prior to PnO DBS, the ictal slow waves were accompanied by alternating UP and DOWN states of neuronal firing (Fig. 2), similar to those seen under deep anesthesia and sleep (35). During and after PnO DBS, tonic, desynchronized MUA was seen (Fig. 2, Fig. 4 A), similar to activity described previously for lightly anesthetized or awake states (15). Autocorrelograms for the baseline epoch exhibited desynchronous characteristics (Fig. 4 B left) whereas autocorrelograms for the ictal pre-DBS epoch showed periodic firing (Fig. 4 B middle). PnO DBS was associated with a reversion of the

autocorrelogram to a desynchronous state (Fig. 4 B right). Group analysis revealed that mean peak correlation values for the first period (see Methods) were significantly higher for the ictal pre-DBS epoch compared to both the baseline ($n= 8$; 1 excluded due to poor MUA signal; $p < 0.0001$) and the ictal DBS ($n= 8$; $p < 0.0001$) epochs (p values Bonferroni-Holm corrected; Fig. 4 C). PnO DBS effectively decreased the degree of correlation to baseline levels such that there was no statistically significant difference between those two epochs ($n= 8$; $p= 0.83$).

Mean spiking rate was also decreased during the transition from tonic firing at baseline to phasic firing during focal limbic seizures (Fig. 4 D, Ictal Pre-DBS). PnO DBS restored the cortical spiking rate to near baseline levels in the ictal and postictal periods, with significantly higher spiking rates than sham in the ictal and postictal DBS epochs ($n= 8$; $p= 0.005$, $p= 0.03$ respectively, Bonferroni-Holm corrected; Fig. 4 D), and a non-significant trend to persistent increased firing in the postictal post-DBS epoch as well (Fig. 4 D).

Cortical physiological arousal with PnO stimulation during focal limbic seizures in awake animals led to minimal improvement in behavior

We next aimed to determine if PnO DBS in the ictal and post ictal states would translate to behavioral signs of arousal. In awake-behaving animals we again used 2 s, 60 Hz hippocampal stimulation to induce focal limbic seizures, accompanied by cortical slow waves as well as behavioral arrest (Supp. 3 A, B). These slow waves were similar to those observed in the LOFC as the animal was naturally sleeping or under deep ketamine/xylazine anesthesia. At least 5 seconds after seizure onset, during which time it was determined that there was no secondary

generalization of the seizure, we stimulated bilateral PnO (current titrated individually per animal; range 70 – 400 μ A) or delivered a 0.2 μ A sham stimulus. The decreases in low-frequency power during PnO DBS in the awake chronically implanted animals (Supp. Fig 3 A, B) resembled the effect of stimulation in the acute preparation. Group analysis demonstrated decreased low-frequency power during and after PnO stimulation (Supp. 3 C), which remained significantly lower than sham controls during the ictal DBS, postictal DBS, and postictal post-DBS epoch (n= 8; Supp. 3 D). While we observed that stimulation abolished ictal slow waves in the cortical LFP during and after DBS, the degree of behavioral recovery, as measured by spontaneous exploratory behavior, was not significant (n= 8, p= 0.17). We noted that application of similar PnO DBS stimulus amplitudes (up to 400 μ A) to awake animals without seizures was capable of interrupting motor activity (data not shown). Therefore we sought an approach to augment the cortical physiological arousal produced by PnO DBS, while using lower PnO stimulus amplitudes in the hopes of also providing behavioral benefit.

Dual-site CL and PnO stimulation improves cortical physiological arousal during focal limbic seizures

Because prior work had suggested an important role for the central lateral intralaminar thalamic nucleus (CL) in modulating arousal following focal limbic and secondarily generalized seizures (13, 14), we decided to stimulate this region. CL stimulation alone at 400 μ A did not significantly decrease cortical slowing during the ictal period (Supp. 4). However, combined CL and PnO stimulation enabled us to reduce the PnO stimulation current by 47% (mean PnO

current = $150 \pm 25 \mu\text{A}$ in PnO alone versus $79 \pm 9 \mu\text{A}$ in dual-site stimulation; $p= 0.01$) while robustly abolishing slow waves during the ictal and postictal periods (Fig. 5).

In group analyses, dual-site CL and PnO DBS resembled the effects of stimulating PnO alone by markedly reducing both ictal and postictal cortical slow waves in awake behaving animals (Fig. 6 A, B). Delta-band power in the ictal DBS epoch was significantly decreased compared to the ictal pre-DBS epoch ($-87.59 \pm 0.87\%$; $n= 6$; $p< 0.0001$, Bonferroni-Holm corrected) as well as compared to sham DBS (Fig. 6 B, C). Postictal cortical slowing remained elevated in sham controls but was significantly reduced with dual-site DBS, restoring cortical activity to near baseline levels (Fig. 6 B, D). Notably, seizure duration remained unchanged between DBS ($52.6 \pm 13.5 \text{ s}$; $n=6$) and sham controls ($44.8 \pm 8.9 \text{ s}$; $n= 7$; $p= 0.63$).

We noted comparable decreases in cortical slow waves with dual-site stimulation without seizures, under anesthesia and from naturally occurring sleep (data not shown).

Dual-site CL and PnO stimulation markedly improves behavioral arousal during focal limbic seizures

Focal limbic seizures were characterized by behavioral arrest with appearance of minor automatisms as previously described (15). However, with dual-site bilateral DBS in awake animals during focal limbic seizures, we observed a marked improvement in normal exploratory behaviors (Fig. 7 A; see also Supp. Video 1). Ratings were performed by two observers with high interobserver reliability ($\kappa = 0.97$). Dual-site CL + PnO DBS restored normal cortical

function and enabled animals to exhibit normal awake behaviors including relaxed forepaw and hindpaw ambulation and exploration of the sides of the cage despite ongoing hippocampal seizure activity (Supp. Video 1). Normal exploratory behaviors were significantly increased during ictal compared to sham DBS ($n=6$; $p < 0.0001$, Bonferroni-Holm corrected; Fig. 7 A) and were not significantly different from pre-seizure baseline. Of note, the dual site DBS did not interfere with normal exploratory behaviors in the post-ictal period (Fig. 7A) and also did not interfere with normal behavior during non-seizure periods (data not shown).

In addition to behavioral arrest during seizures, we often also observed postictal ‘wet-dog-shakes’ which have been previously described in focal rodent limbic seizures (36) accompanied by transient poly-spike discharges on EEG. Postictal wet-dog shakes were also significantly decreased in frequency with dual-site CL + PnO DBS, occurring in only 11.7 % of trials as compared to 91.7 % of sham DBS control trials ($n=6$ animals, $p < 0.0001$) (see Supp. Video 1).

For comparison we also studied effects of dual-site CL + PnO DBS on other states of cortical slow waves and hypoarousal aside from focal limbic seizures, including anesthesia-induced sleep and naturally occurring sleep. We found that dual-site DBS significantly increased exploratory activity ratings as compared to sham DBS during anesthesia ($n=6$; intra-DBS $p < .01$; post-DBS $p < 0.0001$, Bonferroni-Holm corrected; Fig. 7 B) and naturally occurring sleep ($n=6$; intra-DBS $p < 0.01$; post-DBS $p < 0.0001$, Bonferroni-Holm corrected; Fig. 7 C). Animals also showed a significant reduction of slow wave activity in response to the DBS, demonstrating a

physiological transition to an awake state during their exploratory behaviors, before eventually returning to sleep or falling back under anesthesia (data not shown).

Discussion

We have found that dual-site stimulation of subcortical arousal in the thalamus and rostral pons can reverse the adverse effects of focal limbic seizures on conscious arousal, increasing cortical physiological arousal and behavioral responsiveness in the ictal and postictal periods.

Stimulation of PnO alone restored an awake-like cortical state during and after DBS under deep anesthesia, as well as ictally and postictally. This same PnO stimulation in awake-behaving animals yielded similar electrophysiological results, however there was no evidence of behavioral improvement. Stimulation of thalamic CL alone produced cortical physiological arousal under deep anesthesia and postictally (13) but was ineffective in preventing cortical slow waves during seizures. By combining these two targets through dual-site CL + PnO stimulation, we achieved both electrophysiological and behavioral improvement during focal limbic seizures. To our knowledge, these results are the first preclinical data of deep brain stimulation improving ictal level of conscious arousal.

The findings reported here support a model in which serial and/or parallel subcortical arousal systems are depressed during focal limbic seizures (Fig. 1A). The arousal function of these systems can be restored by multi-site stimulation, providing a more potent synergistic effect on cortical circuits than stimulation at a single node of the network (Fig. 1B). This strategy for

multi-site stimulation of subcortical arousal may benefit not only epilepsy, but other disorders of consciousness including traumatic brain injury, stroke, or other states of chronically depressed level of consciousness.

The specific sites stimulated in this study are integral nodes in subcortical arousal, however additional targets could be considered in future investigations (32). The pontine reticular formation and in particular PnO has been implicated in the modulation of spontaneous activity, REM sleep, and wakefulness with sometimes disparate conclusions as to its role. Early studies concluded that the pontine reticular formation had no role in spontaneous activity (37), while some recent evidence suggests that it definitively contributes to behavioral state and cortical slow-wave regulation (38). Multiple drug infusion studies have solidified its role as a sleep regulatory region (39-42). More recently, stimulation of the PnO has been shown to induce cortical desynchronization in lightly anesthetized rats as well as increase functional connectivity to basal forebrain-paralimbic structures such as the nucleus basalis of Meynert (43).

Likewise, the intralaminar thalamus has also been implicated in the modulation of sleep-wake state, anesthesia, level of awareness, and attention (25, 35, 44-46). Thalamic CL stimulation in an exemplary patient suffering chronic posttraumatic encephalopathy with minimally conscious state yielded stimulation-dependent arousal and improved functional outcomes including arousal (29). Stimulation of CL has been previously shown by our group to induce cortical desynchronization under anesthesia and to improve arousal in freely-behaving animals in the postictal period (13). Here we demonstrate its insufficiency at producing cortical

desynchronization during seizure when stimulated alone, and feel that this reflects a more widespread, multi-pathway inhibition of subcortical arousal ictally than is present postictally. Further evidence of the multi-pathway subcortical arousal network can be seen when contrasting the effects of single-site with dual-site stimulation; cortical desynchronization was more robust and required lower amplitudes in both loci with dual stimulation as compared to single site stimulation. With stimulation of either locus alone being insufficient, but stimulation of both being necessary to produce the electrophysiological and behavioral correlates of restored consciousness, this supports the idea of multiple, complexly overlapping arousal pathways that have differential effects on consciousness depending on the combination of active nodes and the states during which they become active. In the context of previous studies and rapidly improving responsive neurostimulation and DBS technology, our results offer a feasible new strategy for addressing the loss of consciousness in medically refractory focal epilepsy, with clear implications for other disorders of consciousness.

Further studies are needed to explore optimal stimulation paradigms and parameters. For example, future investigation may include stimulation concurrent with, or even before, seizure onset, which was not done during the present studies to allow for assessment of secondary generalization prior to therapeutic stimulus delivery. The present study specifically investigated focal limbic seizures without generalization although in previous work we found a beneficial effect on arousal by stimulating CL in the postictal period after secondarily generalized seizures (13). In focal seizures without generalization we also found a beneficial effect on cortical physiological arousal in the postictal period, although we did not observe significant postictal

deficits. Thus behavioral benefits could not be observed in the postictal period. Further studies using more detailed behavioral testing with stimulus/response paradigms may enable a more nuanced understanding of any cognitive improvements provided by DBS in the ictal and postictal periods. Other stimulation parameters such as frequency, pulse-width, amplitude, duration, and stimulation pattern (e.g. intermittent vs. continuous), also require further investigation. Furthermore, although gamma band activity was partly obscured by the stimulus frequency ranges used in the present study it could be of interest to investigate changes in high frequency gamma band cortical activity as an additional marker of cortical activation in future investigations. Of particular interest is recent data showing that optogenetic activation of brainstem cholinergic neurons in the pedunculo-pontine tegmental nucleus of rats during focal limbic seizures is capable of improving cortical physiological arousal (47). In addition, optogenetic stimulation of GABAergic and glycinergic axon fibers from the pontine reticular formation has been shown to cause intralaminar thalamic inhibition, leading to behavioral arrest and interruption of awake-like cortical activity in freely moving mice (38) further solidifying a role for subcortical interactions in modulation of arousal. Whereas optogenetic's mechanism-of-action provides an elegant dissection of specific neuronal contributions to network function, the complex and potentially non-specific mechanisms of electrical stimulation prohibits us from fully identifying which neuronal populations are being activated or deactivated. Furthermore, *en passant* fibers, perhaps from other subcortical arousal systems like the deep mesencephalic or pedunculo-pontine nuclei are surely affected in an unknown, possibly contributory way. On the other hand, the relatively broad and potentially robust effects of electrical stimulation, a mode of neuromodulation already in wide clinical use, clearly

allow rapid practical clinical translation especially when coupled with current responsive neurostimulation paradigms (48-52).

With regard to alternative targets, other subcortical arousal structures have been investigated within the context of sleep, anesthesia, Parkinson's and other disorders, and have shown varying effects on level of arousal (32). While therapeutic electrodes have been implanted in infratentorial targets very near PnO in humans, such as the pedunculopontine nucleus (53, 54), a supratentorial target may offer a decreased surgical risk profile. Of note, the nucleus basalis is supratentorial, is in the ascending projection pathway of PnO, and has widespread cholinergic and non-cholinergic arousal connections with the neocortex (14, 16, 34, 43) making it a promising potential future target for stimulation.

Impairment from loss of consciousness during seizures is a major contributor to the morbidity and mortality associated with the epilepsies (1, 2, 55, 56). The mechanisms of subcortical impairment causing loss of consciousness during seizures are also implicated in the cardiorespiratory dysfunction leading to sudden unexpected death in epilepsy (SUDEP) (57, 58). Furthermore the decreased productivity, decreased quality of life and social stigma associated with loss of consciousness highlight it as a clinical attribute worthy of being addressed.

Continuous DBS of the anterior nucleus of the thalamus as well as NeuroPace-based responsive neuromodulation of epileptogenic foci have thus far been focused solely on decreasing seizure frequency (5, 59). For patients lacking complete seizure control i.e. patients with medically and surgically refractory epilepsy, epileptic foci in eloquent areas, or health conditions which

contraindicate a large resective surgery, improving their level of consciousness during seizures with DBS could have a dramatic impact on their quality of life as well as their overall mortality risk. Current stereotactic surgery on brain areas in the same or very close proximity to those discussed here have been proven safe and effective in other neurological disorders (29, 53, 54, 60). We expect the present results to set the stage for rapid translation of this preclinical data into a new therapeutic strategy to improve quality of life for people with epilepsy.

Acknowledgements

I thank Abhijeet Gummadavelli for graciously giving me data on 3 CL-implanted animals. I thank Chanthia Ma and Mengran Liu for their enthusiasm, willingness to learn, and help with histology. I thank Dr. Cian McCafferty, Dr. Nicholas Schiff, Dr. Jon Willie, Dr. Robert Gross, and Dr. Jason Gerrard for insightful comments and critiques throughout the entire process. I thank Dr. James O. McNamara for helpful comments and for making us aware of the behavior and physiology of postictal wet-dog shakes in rodent limbic seizures. I thank Abbie Kundishora for illustrations used on the cover and in figure 7. And finally, I deeply thank Dr. Hal Blumenfeld for sharing his genius, not only as it applies to science, but as it applies to living healthily, morally, and harmoniously. This work was supported by Howard Hughes Medical Institute – Citizens United for Research in Epilepsy Medical Student Research Fellowship, and by National Institutes of Health R01 NS066974, R21 NS083783 and P30 NS052519.

References

1. Vickrey BG, Berg AT, Sperling MR, Shinnar S, Langfitt JT, Bazil CW, Walczak TS, Pacia S, Kim S, and Spencer SS. Relationships between seizure severity and health-related quality of life in refractory localization-related epilepsy. *Epilepsia*. 2000;41(6):760-4.
2. Sander JW. The epidemiology of epilepsy revisited. *Current opinion in neurology*. 2003;16(2):165-70.
3. Blumenfeld H. Impaired consciousness in epilepsy. *The Lancet Neurology*. 2012;11(9):814-26.
4. Englot DJ, Chang EF, and Auguste KI. Vagus nerve stimulation for epilepsy: a meta-analysis of efficacy and predictors of response. *Journal of neurosurgery*. 2011;115(6):1248-55.
5. Salanova V, Witt T, Worth R, Henry TR, Gross RE, Nazzaro JM, Labar D, Sperling MR, Sharan A, Sandok E, et al. Long-term efficacy and safety of thalamic stimulation for drug-resistant partial epilepsy. *Neurology*. 2015;84(10):1017-25.
6. Heck CN, King-Stephens D, Massey AD, Nair DR, Jobst BC, Barkley GL, Salanova V, Cole AJ, Smith MC, Gwinn RP, et al. Two-year seizure reduction in adults with medically intractable partial onset epilepsy treated with responsive neurostimulation: final results of the RNS System Pivotal trial. *Epilepsia*. 2014;55(3):432-41.
7. Blumenfeld H. *The Neuroanatomy of Consciousness: Cognitive Neurosciences and Neuropathology*. NY: Elsevier, Academic Press; 2015.
8. Blumenfeld H. *Higher order cerebral function*. Sunderland, MA: Sinauer Assoc Publ.; 2010.
9. Posner JB, Schiff ND, Plum F. *Plum and Posner's Diagnosis of Stupor and Coma*. USA: Oxford University Press; 2007.
10. Giacino JT, Fins JJ, Laureys S, and Schiff ND. Disorders of consciousness after acquired brain injury: the state of the science. *Nature reviews Neurology*. 2014;10(2):99-114.
11. Schiff ND, and Laureys S. Disorders of consciousness. Preface. *Ann N Y Acad Sci*. 2009;1157(ix-xi).
12. Norden AD, and Blumenfeld H. The role of subcortical structures in human epilepsy. *Epilepsy & behavior : E&B*. 2002;3(3):219-31.
13. Gummadavelli A, Motelow JE, Smith N, Zhan Q, Schiff ND, and Blumenfeld H. Thalamic stimulation to improve level of consciousness after seizures: Evaluation of electrophysiology and behavior. *Epilepsia*. 2015;56(1):114-24.
14. Motelow JE, Li W, Zhan Q, Mishra AM, Sachdev RN, Liu G, Gummadavelli A, Zayyad Z, Lee HS, Chu V, et al. Decreased subcortical cholinergic arousal in focal seizures. *Neuron*. 2015;85(3):561-72.
15. Englot DJ, Mishra AM, Mansuripur PK, Herman P, Hyder F, and Blumenfeld H. Remote effects of focal hippocampal seizures on the rat neocortex. *The Journal of neuroscience : the official journal of the Society for Neuroscience*. 2008;28(36):9066-81.
16. Englot DJ, Modi B, Mishra AM, DeSalvo M, Hyder F, and Blumenfeld H. Cortical deactivation induced by subcortical network dysfunction in limbic seizures. *The Journal*

- of neuroscience : the official journal of the Society for Neuroscience*. 2009;29(41):13006-18.
17. Li W, Motelow JE, Zhan Q, Hu YC, Kim R, Chen WC, and Blumenfeld H. Cortical network switching: possible role of the lateral septum and cholinergic arousal. *Brain Stimul*. 2015;8(1):36-41.
 18. Englot DJ, Yang L, Hamid H, Danielson N, Bai X, Marfeo A, Yu L, Gordon A, Purcaro MJ, Motelow JE, et al. Impaired consciousness in temporal lobe seizures: role of cortical slow activity. *Brain : a journal of neurology*. 2010;133(Pt 12):3764-77.
 19. Blumenfeld H, Rivera M, McNally KA, Davis K, Spencer DD, and Spencer SS. Ictal neocortical slowing in temporal lobe epilepsy. *Neurology*. 2004;63(6):1015-21.
 20. Blumenfeld H, McNally KA, Vanderhill SD, Paige AL, Chung R, Davis K, Norden AD, Stokking R, Studholme C, Novotny EJ, et al. Positive and negative network correlations in temporal lobe epilepsy. *Cerebral Cortex*. 2004;14(8):892-902.
 21. Cunningham C, Chen WC, Shorten A, McClurkin M, Choezom T, Schmidt CP, Chu V, A. B, Best C, Chapman M, et al. Impaired consciousness in partial seizures is bimodally distributed. *Neurology*. 2014;82(19):1736-44.
 22. Brown EN, Lydic R, and Schiff ND. General anesthesia, sleep, and coma. *The New England journal of medicine*. 2010;363(27):2638-50.
 23. Zhan Q BG, Motelow JE, Andrews J, Vitkovskiy P, Chen WC, Serout F, Gummadavelli A, Kundishora A, Furman M, Li W, Bo X, Richerson GB, Blumenfeld H. Impaired serotonergic brainstem function during and following seizures. *The Journal of neuroscience : the official journal of the Society for Neuroscience*. 2016IN PRESS).
 24. Penfield W. Epilepsy and surgical therapy. *Arch Neuro Psychiatr*. 1936;36(3):449-84.
 25. Van der Werf YD, Witter MP, and Groenewegen HJ. The intralaminar and midline nuclei of the thalamus. Anatomical and functional evidence for participation in processes of arousal and awareness. *Brain research Brain research reviews*. 2002;39(2-3):107-40.
 26. Sturm V, Kuhner A, Schmitt HP, Assmus H, and Stock G. Chronic electrical stimulation of the thalamic unspecific activating system in a patient with coma due to midbrain and upper brain stem infarction. *Acta neurochirurgica*. 1979;47(3-4):235-44.
 27. Hassler R, Ore GD, Dieckmann G, Bricolo A, and Dolce G. Behavioural and EEG arousal induced by stimulation of unspecific projection systems in a patient with post-traumatic apallic syndrome. *Electroencephalography and clinical neurophysiology*. 1969;27(3):306-10.
 28. McLardy T, Ervin F, Mark V, Scoville W, and Sweet W. Attempted inset-electrodes-arousal from traumatic coma: neuropathological findings. *Transactions of the American Neurological Association*. 1968;93(25-30).
 29. Schiff ND, Giacino JT, Kalmar K, Victor JD, Baker K, Gerber M, Fritz B, Eisenberg B, Biondi T, O'Connor J, et al. Behavioural improvements with thalamic stimulation after severe traumatic brain injury. *Nature*. 2007;448(7153):600-3.
 30. Morison RS, Dempsey EW, and Morison BR. Cortical responses from electrical stimulation of the brain stem. *Am J Physiol*. 1941;131(3):0732-43.
 31. Moruzzi G, and Magoun HW. Brain stem reticular formation and activation of the EEG. *Electroencephalography and clinical neurophysiology*. 1949;1(4):455-73.

32. Gummadvelli A, Kundishora AJ, Willie JT, Andrews JP, Gerrard JL, Spencer DD, and Blumenfeld H. Neurostimulation to improve level of consciousness in patients with epilepsy. *Neurosurgical focus*. 2015;38(6):E10.
33. Paxinos G, and Watson C. *The rat brain in stereotaxic coordinates*. San Diego: Academic Press; 1998.
34. Englot DJ, and Blumenfeld H. Consciousness and epilepsy: why are complex-partial seizures complex? *Progress in brain research*. 2009;177(147-70).
35. Steriade M, McCormick DA, and Sejnowski TJ. Thalamocortical oscillations in the sleeping and aroused brain. *Science (New York, NY)*. 1993;262(5134):679-85.
36. Dyer RS, Swartzwelder HS, Eccles CU, and Annau Z. Hippocampal afterdischarges and their post-ictal sequelae in rats: a potential tool for assessment of CNS neurotoxicity. *Neurobehavioral toxicology*. 1979;1(1):5-19.
37. Lynch G. Behavioral excitability and the giant-celled pontine reticular formation (nucleus reticularis pontis oralis). *Brain research*. 1971;32(2):449-53.
38. Giber K, Diana MA, Plattner VM, Dugue GP, Bokor H, Rousseau CV, Magloczky Z, Havas L, Hangya B, Wildner H, et al. A subcortical inhibitory signal for behavioral arrest in the thalamus. *Nature neuroscience*. 2015;18(4):562-8.
39. Marks GA, and Birabil CG. Enhancement of rapid eye movement sleep in the rat by cholinergic and adenosinergic agonists infused into the pontine reticular formation. *Neuroscience*. 1998;86(1):29-37.
40. Ahnaou A, Basille M, Gonzalez B, Vaudry H, Hamon M, Adrien J, and Bourgin P. Long-term enhancement of REM sleep by the pituitary adenylyl cyclase-activating polypeptide (PACAP) in the pontine reticular formation of the rat. *The European journal of neuroscience*. 1999;11(11):4051-8.
41. Bourgin P, Escourrou P, Gaultier C, and Adrien J. Induction of rapid eye movement sleep by carbachol infusion into the pontine reticular formation in the rat. *Neuroreport*. 1995;6(3):532-6.
42. Lopez-Rodriguez F, Kohlmeier K, Morales FR, and Chase MH. State dependency of the effects of microinjection of cholinergic drugs into the nucleus pontis oralis. *Brain research*. 1994;649(1-2):271-81.
43. Pillay S, Liu X, Baracskey P, and Hudetz AG. Brainstem stimulation increases functional connectivity of basal forebrain-paralimbic network in isoflurane-anesthetized rats. *Brain connectivity*. 2014;4(7):523-34.
44. Kinomura S, Larsson J, Gulyas B, and Roland PE. Activation by attention of the human reticular formation and thalamic intralaminar nuclei. *Science (New York, NY)*. 1996;271(5248):512-5.
45. Jones EG. The thalamic matrix and thalamocortical synchrony. *Trends in neurosciences*. 2001;24(10):595-601.
46. Steriade M, Contreras D, Amzica F, and Timofeev I. Synchronization of fast (30-40 Hz) spontaneous oscillations in intrathalamic and thalamocortical networks. *The Journal of neuroscience : the official journal of the Society for Neuroscience*. 1996;16(8):2788-808.
47. Furman M, Zhan Q, McCafferty C, Lerner BA, Motelow JE, Meng J, Ma C, Buchanan GF, Witten IB, Deisseroth K, et al. Optogenetic Stimulation of Cholinergic Brainstem Neurons During Focal Limbic Seizures: Effects of Cortical Physiology. *Epilepsia*. 2015;In Press(

48. Al-Otaibi FA, Hamani C, and Lozano AM. Neuromodulation in epilepsy. *Neurosurgery*. 2011;69(4):957-79; discussion 79.
49. Ben-Menachem E, and Krauss GL. Epilepsy: responsive neurostimulation-modulating the epileptic brain. *Nature reviews Neurology*. 2014;10(5):247-8.
50. Fountas KN, Smith JR, Murro AM, Politsky J, Park YD, and Jenkins PD. Implantation of a closed-loop stimulation in the management of medically refractory focal epilepsy: a technical note. *Stereotactic and functional neurosurgery*. 2005;83(4):153-8.
51. Anderson WS, Kossoff EH, Bergey GK, and Jallo GI. Implantation of a responsive neurostimulator device in patients with refractory epilepsy. *Neurosurgical focus*. 2008;25(3):E12.
52. Morrell MJ, and Group RNSSiES. Responsive cortical stimulation for the treatment of medically intractable partial epilepsy. *Neurology*. 2011;77(13):1295-304.
53. Mazzone P, Lozano A, Stanzione P, Galati S, Scarnati E, Peppe A, and Stefani A. Implantation of human pedunculo-pontine nucleus: a safe and clinically relevant target in Parkinson's disease. *Neuroreport*. 2005;16(17):1877-81.
54. Plaha P, and Gill SS. Bilateral deep brain stimulation of the pedunculo-pontine nucleus for Parkinson's disease. *Neuroreport*. 2005;16(17):1883-7.
55. Charidimou A, and Selai C. The effect of alterations in consciousness on quality of life (QoL) in epilepsy: searching for evidence. *Behavioural neurology*. 2011;24(1):83-93.
56. Chen WC, Chen EY, Gebre RZ, Johnson MR, Li N, Vitkovskiy P, and Blumenfeld H. Epilepsy and driving: potential impact of transient impaired consciousness. *Epilepsy & behavior : E&B*. 2014;30(50-7).
57. Massey CA, Sowers LP, Dlouhy BJ, and Richerson GB. Mechanisms of sudden unexpected death in epilepsy: the pathway to prevention. *Nature reviews Neurology*. 2014;10(5):271-82.
58. Devinsky O. Sudden, unexpected death in epilepsy. *The New England journal of medicine*. 2011;365(19):1801-11.
59. Morrell MJ, and Halpern C. Responsive Direct Brain Stimulation for Epilepsy. *Neurosurg Clin N Am*. 2016;27(1):111-21.
60. Giacino J, Fins JJ, Machado A, and Schiff ND. Central thalamic deep brain stimulation to promote recovery from chronic posttraumatic minimally conscious state: challenges and opportunities. *Neuromodulation : journal of the International Neuromodulation Society*. 2012;15(4):339-49.
61. Jang SH, Lim HW, and Yeo SS. The neural connectivity of the intralaminar thalamic nuclei in the human brain: a diffusion tensor tractography study. *Neuroscience letters*. 2014;579(140-4).

Figures

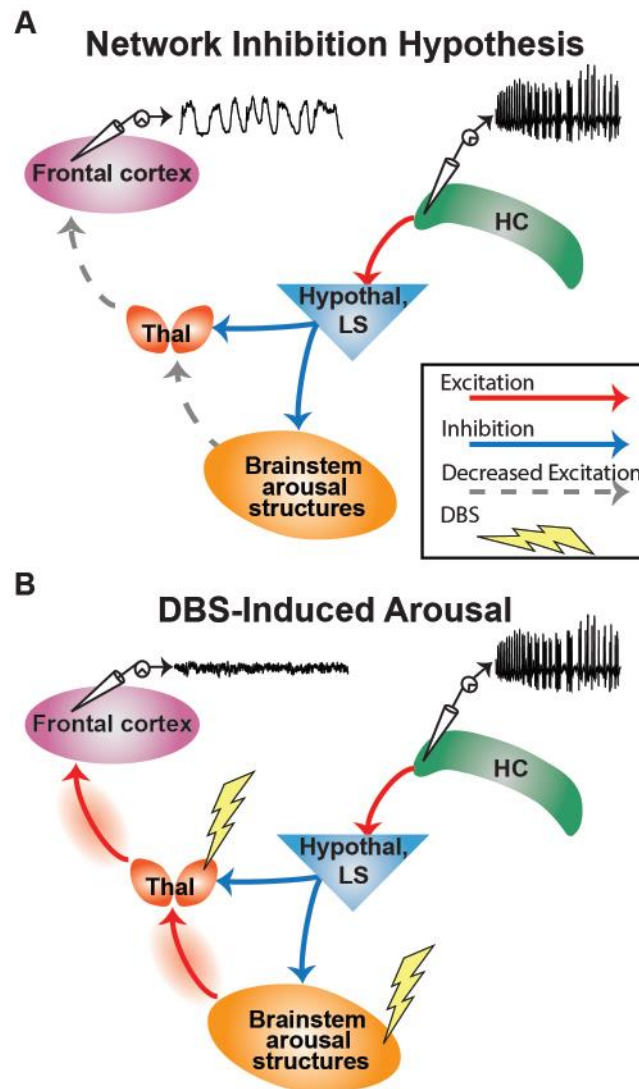


Figure 1. The Network Inhibition Hypothesis and Proposed Therapeutic Intervention. (A)

Schematized representation of focal hippocampal seizure causing cortical slow waves and loss of consciousness. Seizure activity propagates via excitatory projections to the hypothalamus (Hypothal) and lateral septum (LS). This activates neurons with inhibitory projections to numerous subcortical arousal structures including the midbrain and pontine reticular formation in the upper brainstem and the intralaminar thalamus (Thal). Inactivating these arousal

structures has the effect of decreasing excitatory input to the cortex (Frontal cortex, as well as other cortical areas), thus allowing it to fall into a sleep-like state. This is electrophysiologically characterized by large amplitude, low frequency 'slow-waves.' **(B)** Dual-site deep brain stimulation (DBS) in the inhibited brainstem arousal structures and thalamus during focal hippocampal seizures restores excitatory input to the cortex, restoring awake-like cortical fast activity and improving conscious arousal.

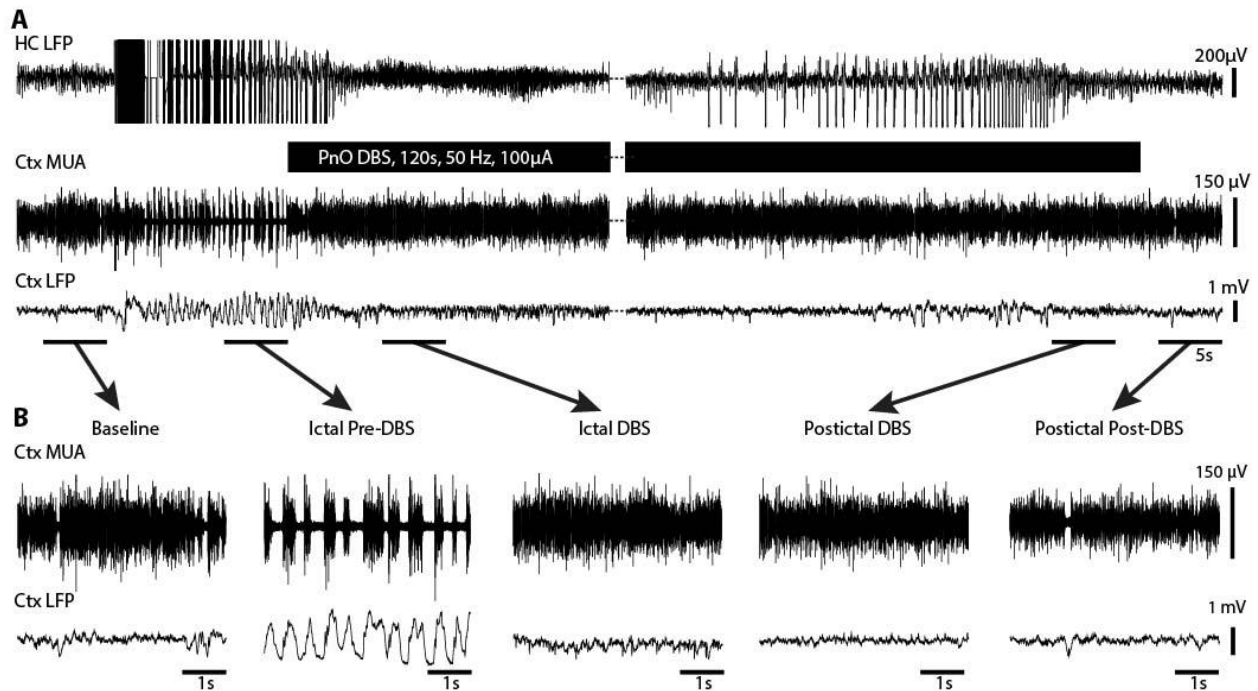


Figure 2. Cortical physiological arousal with PnO DBS in a focal limbic seizure. (A) Pontine nucleus oralis DBS during focal limbic seizure in a lightly anesthetized animal decreases slowing in lateral orbital frontal cortex. Seizure was induced by 2 s, 60 Hz stimulation of hippocampus (HC). Break in recording of 51 s, during which seizure and DBS continue, enables display of the post-DBS time period. Total DBS duration was 120 s. **(B)** 5-second-long magnified insets of marked baseline, ictal pre-DBS, ictal DBS, ictal post-DBS, and postictal post-DBS epochs exemplify desynchronized lateral orbital frontal cortical local field potentials (Ctx LFP) intra- and post-DBS. Lateral orbital frontal cortical multi-unit activity (MUA) transitions from phasic firing in the ictal pre-DBS period to tonic firing in response to DBS. After PnO stimulation, cortex remains in desynchronized state and no postictal state ensues.

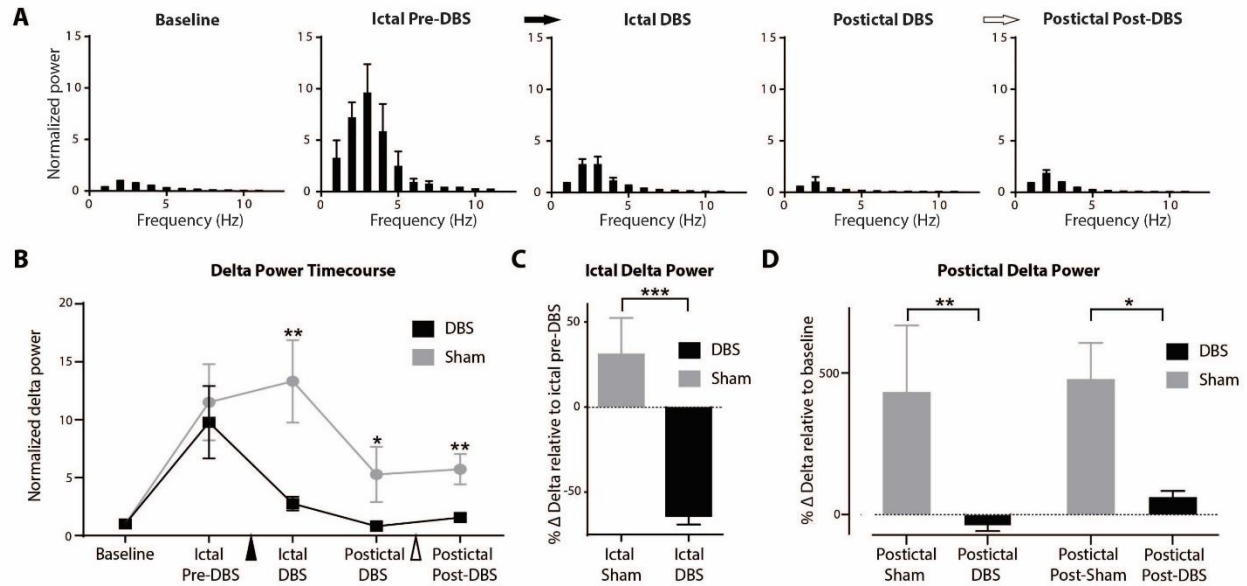


Figure 3. Group local field potential data for PnO DBS during focal limbic seizures under light anesthesia. (A) Ictal pre-DBS low frequency power is increased. PnO DBS decreases this low-frequency power during ictal DBS, postictal DBS, and postictal post-DBS epochs. Black arrow indicates onset and white arrow end of PnO DBS. **(B)** Time course of delta-band (0-4 Hz) power during each epoch compared to sham stimulation. There is a significant difference between DBS and sham conditions during the ictal DBS, postictal DBS, and postictal post-DBS epochs. Black arrowhead indicates onset and white arrowhead end of PnO stimulation. **(C)** Ictal DBS delta-band power relative to the ictal pre-DBS delta-band power is significantly decreased compared to sham controls. **(D)** Postictal DBS and postictal post-DBS delta-band power relative to baseline delta power remains elevated in sham conditions but are returned to near-baseline levels in the DBS conditions. $n = 9$ (DBS), $n = 7$ (Sham) animals. All results are mean \pm SEM. * $p < 0.05$, ** $p < 0.01$, *** $p < 0.001$ Bonferroni-Holm corrected.

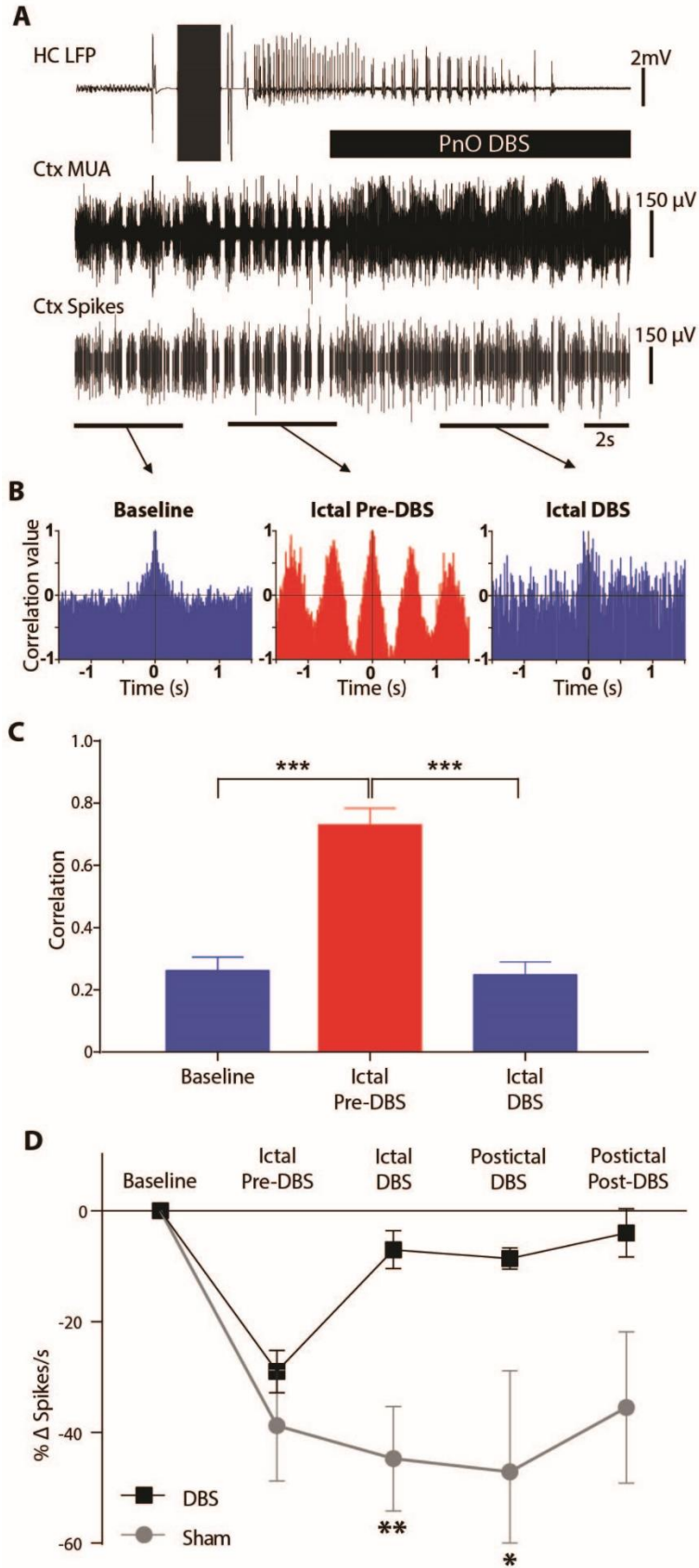


Figure 4. Transition of cortical multi-unit activity from phasic to tonic firing with DBS during focal limbic seizures. (A) Example of PnO stimulation during focal limbic seizure induced by 2 s, 60 Hz stimulation of the hippocampus (HC) under light anesthesia. DBS reverts the phasic UP and DOWN states seen in lateral orbital frontal cortical multiunit activity (Ctx MUA) during the ictal pre-DBS epoch back to tonic desynchronized firing. The bottom-most trace (Ctx Spikes) represents spike-sorted Ctx MUA data. **(B)** Autocorrelograms of the marked epochs demonstrated desynchronized firing in the baseline and ictal DBS epochs and highly phasic firing in the ictal pre-DBS epoch. **(C)** Group average peak correlation for the first period (see Methods) revealed a significant difference between Ictal Pre-DBS and both the Baseline or Ictal DBS epochs. **(D)** Group average spikes per second data demonstrate a large drop in spike rate during focal limbic seizures that is reversed in the DBS case but not in the sham case. There is a significant difference between DBS and sham condition change in spike rate during the ictal DBS and postictal DBS epochs. For C, and D all results are mean \pm SEM; n= 8 animals. Same animals as Figure 3 except for one animal that did not have usable MUA data. *p< 0.05, **p< 0.01, ***p< 0.001, Bonferroni-Holm corrected.

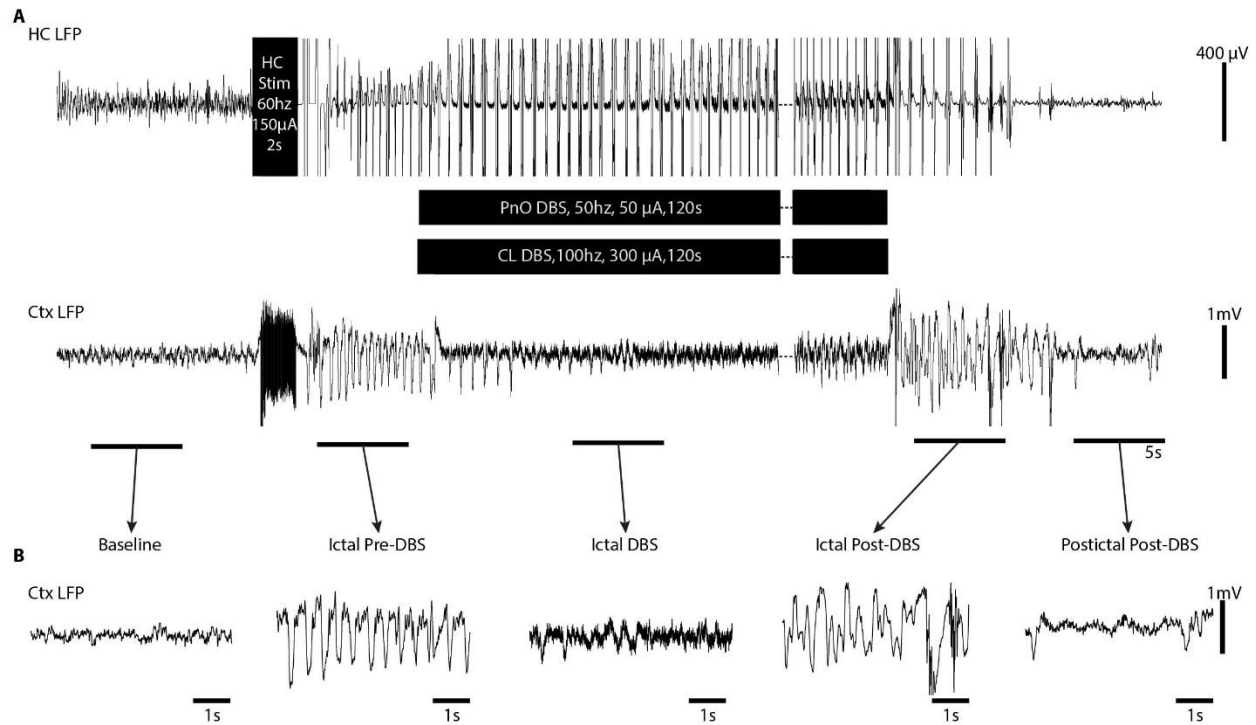


Figure 5. Dual-site stimulation of CL + PnO produces cortical physiological arousal during focal limbic seizure in an awake behaving animal. (A) Combined central lateral thalamic and pontine nucleus oralis DBS during focal limbic seizure in an awake behaving animal decreases slowing in lateral orbital frontal cortical local field potentials (Ctx LFP). Seizure was induced by 2 s, 60 Hz stimulation of hippocampus (HC). Break in recording of 90 s, during which seizure and DBS continue, enables display of the post-DBS time period. Total DBS duration was 120 s. **(B)** 5-second-long magnified insets of marked baseline, ictal pre-DBS, ictal DBS, ictal post-DBS, and postictal post-DBS epochs exemplify desynchronized Ctx LFP intrastimulus. Slowing returns after stimulation ceases while the seizure continues (total seizure duration in this example was longer than the DBS). Postictally, Ctx LFP returns to desynchronized state.

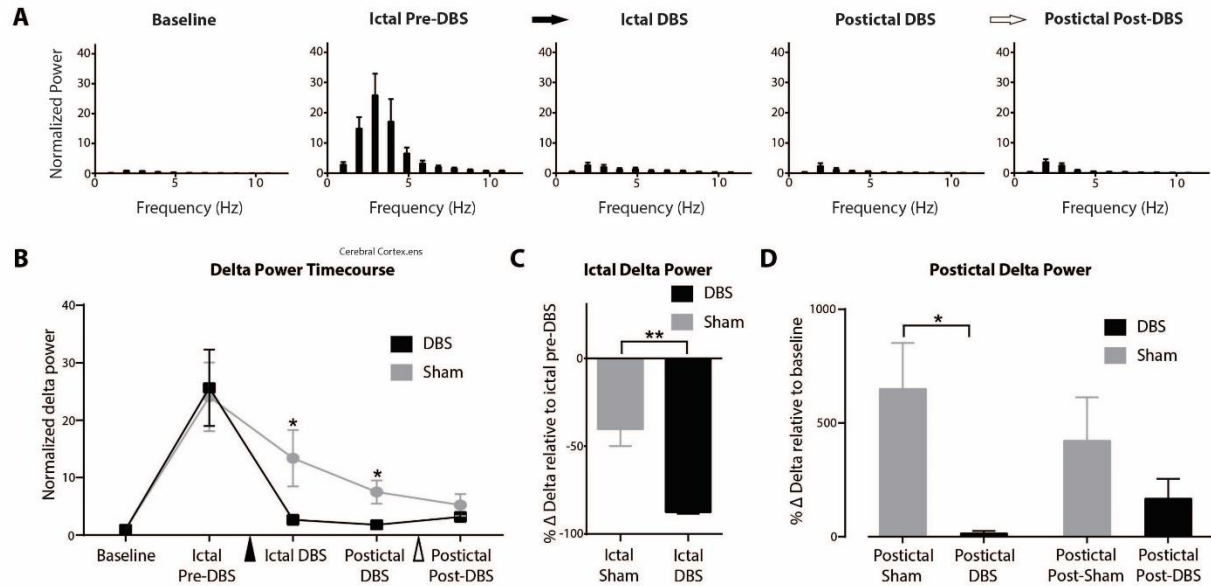


Figure 6. Group data for dual-site CL and PnO stimulation during focal limbic seizures in awake behaving animals. (A) Dual-site CL + PnO DBS decreases low-frequency power during and following focal limbic seizures induced in the awake state. Black arrow indicates onset and white arrow termination of PnO DBS. **(B)** Time course of delta-band (0-4 Hz) power during each time epoch as compared to sham stimulation. There is a significant difference between the DBS and sham conditions during the ictal DBS and postictal DBS epochs. Black arrowhead indicates onset and white arrowhead end of PnO DBS. **(C)** Ictal DBS delta-band power relative to the ictal pre-DBS delta power is significantly decreased compared to sham stimulation. **(D)** Postictal DBS delta band power relative to baseline delta power remains elevated in the sham case and is returned to near-baseline levels in the simulation case. All results are mean \pm SEM; $n=6$ animals. * $p < 0.05$, ** $p < 0.01$, Bonferroni-Holm corrected.

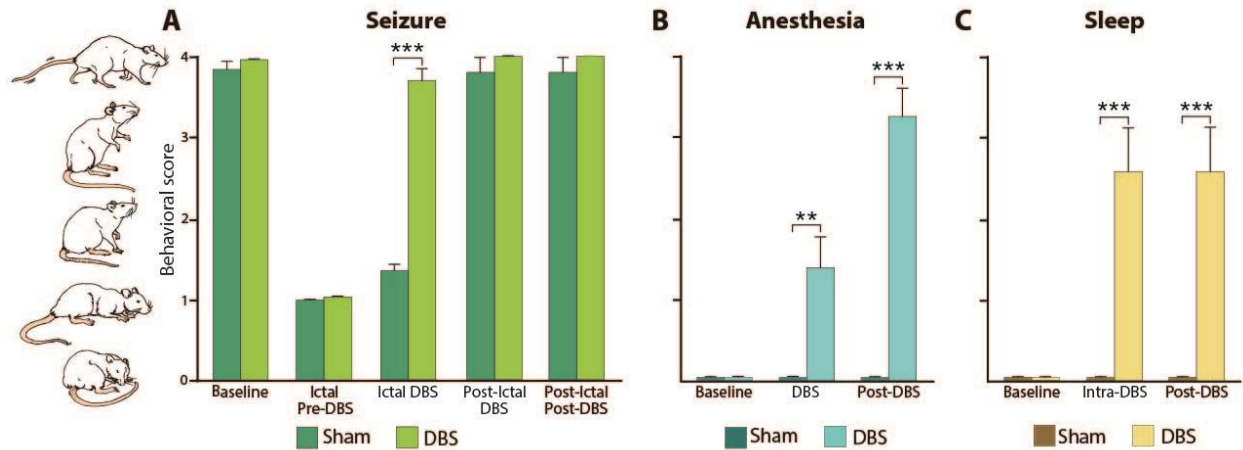
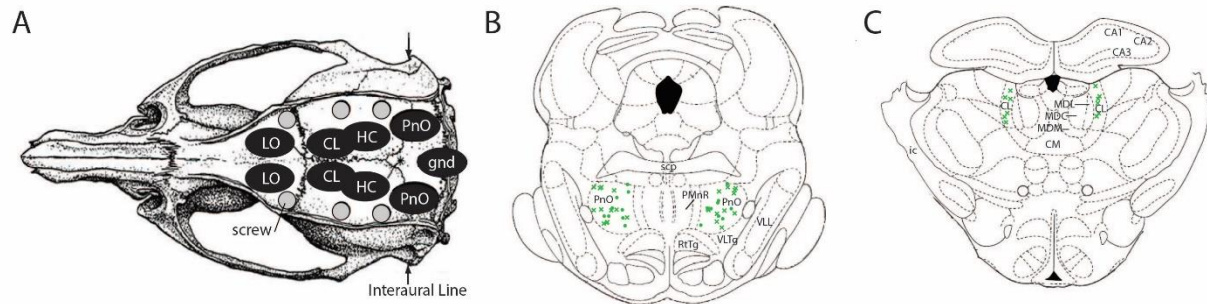


Figure 7. Behavioral arousal with dual-site CL+ PnO DBS during focal limbic seizures, anesthesia-induced sleep, and natural sleep. (A) CL + PnO DBS significantly increased spontaneous exploratory behavior during focal limbic seizures as compared to sham stimulation. $n = 6$ animals. **(B)** CL + PnO DBS significantly increased spontaneous exploratory behavior during the intra- and post-DBS epochs under low-dose anesthesia-induced sleep. $n = 6$ animals. **(C)** CL + PnO stimulation significantly increased spontaneous exploratory behavior during the intra- and post-stimulation epochs during physiological sleep. $n = 6$ animals (same animals as in Figure 6). All data (A-C) are shown as mean \pm SEM. ** $p < 0.01$, *** $p < 0.001$, Bonferroni-Holm corrected.

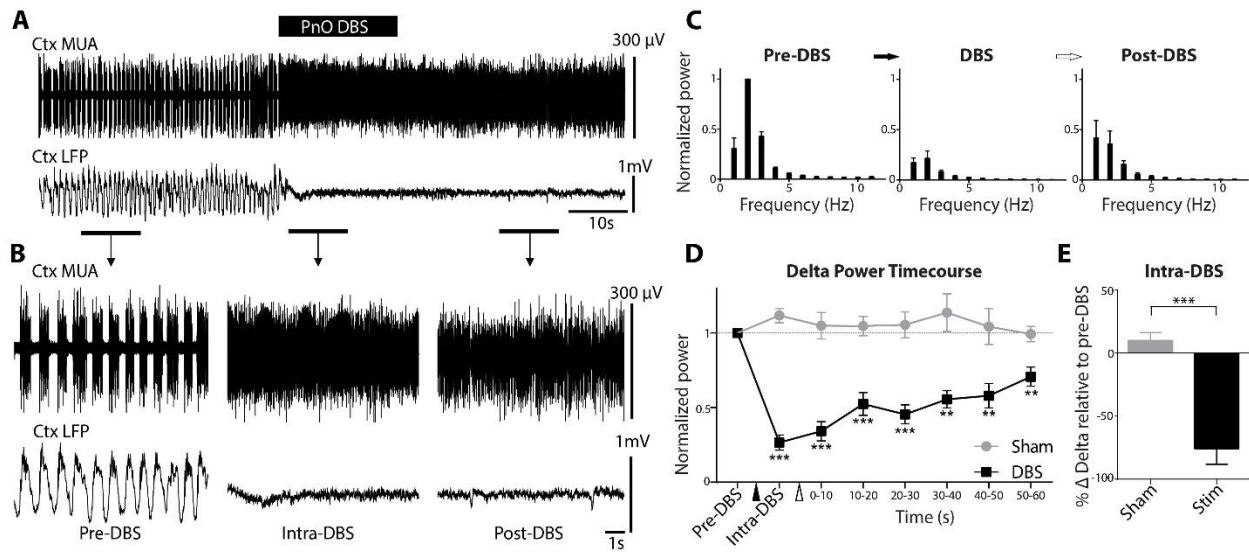


Supplementary Figure 1. Summary of electrode placements (A) Schematic of the dorsal aspect of a rat skull depicting sites of craniotomies (black circles), screw burr holes (gray circles), and ground screw burr hole (gnd). Bilateral or unilateral craniotomies were used depending on the experimental series as explained in the Methods. **(B)** Summary of electrode tip locations in PnO at AP -8.0 mm. (•'s represent acute and x's chronic electrode tip locations) from all experiments included in the present analysis (n= 20 animals). **(C)** Summary of electrode tip locations in CL at AP -2.8 mm from all experiments included in the present analysis (n= 9 animals). Note that although 29 total electrode positions are shown these are from 23 animals total used in all experiments, because 6 animals were used for dual PNO + CL experiments.

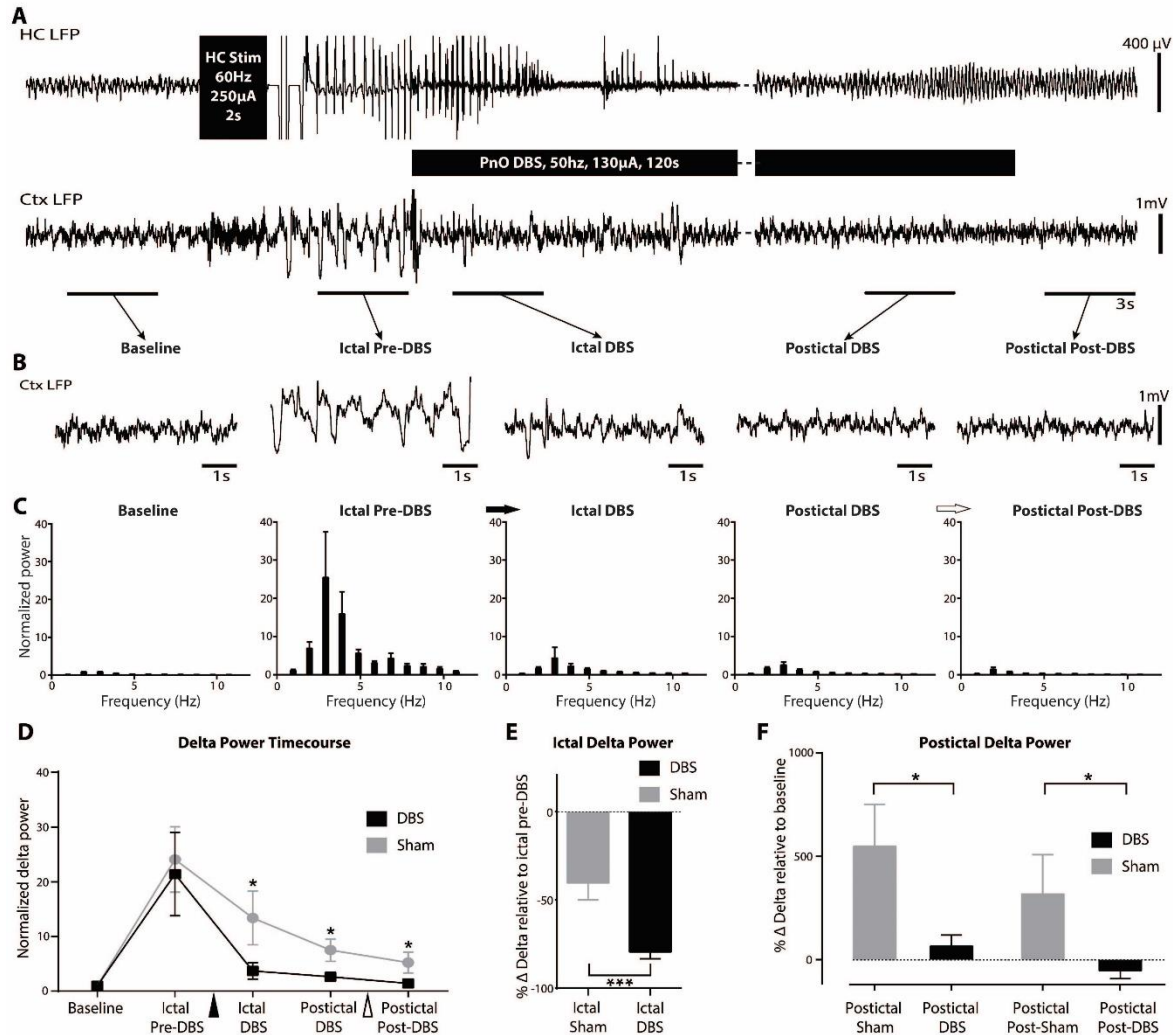
The animals used and excluded in different experiments based on histology can be summarized as follows: For acute PnO deep anesthesia DBS n= 7 (Supp Fig 2); for acute PnO seizure DBS n= 9 (Fig 3). Note that total animals used for PnO anesthesia experiments was 12 because 4 animals were used for both deep anesthesia and seizure experiments. Total animals excluded from PnO anesthesia experiments due to inaccurate electrode placements were 9. For acute CL seizure DBS n= 3 (Supp Fig 4). No animals were excluded so total animals used for CL anesthesia experiments was 3. For chronic PnO seizure DBS n= 8 (Supp Fig 3). For chronic PnO + CL seizure DBS n= 6 (Figs 6, 7). Note that total animals used for chronic experiments was

8 because 8 animals were used in both PnO as well as in PnO + CL experiments. Total animals excluded from chronic experiments due to inaccurate electrode placements were 6.

CA1, cornus ammonis 1; CA2, cornus ammonis 2; CA3, cornus ammonis 3; CL, central lateral intralaminar thalamic nucleus; CM, central medial intralaminar thalamic nucleus; gnd, ground; HC, hippocampus; LO, lateral orbitofrontal cortex; MDC, mediodorsal thalamic nucleus, central part; MDL, mediodorsal thalamic nucleus, lateral part; MDM, mediodorsal thalamic nucleus, medial part; PMnR, paramedian raphe nucleus; PnO, pontine reticular nucleus, oral part; RtTg, reticulotegmental nucleus of the pons; scp, superior cerebellar peduncle; VLL, ventral nucleus of the lateral lemniscus. Base images for A – C reproduced with permission from Paxinos and Watson, 1998.



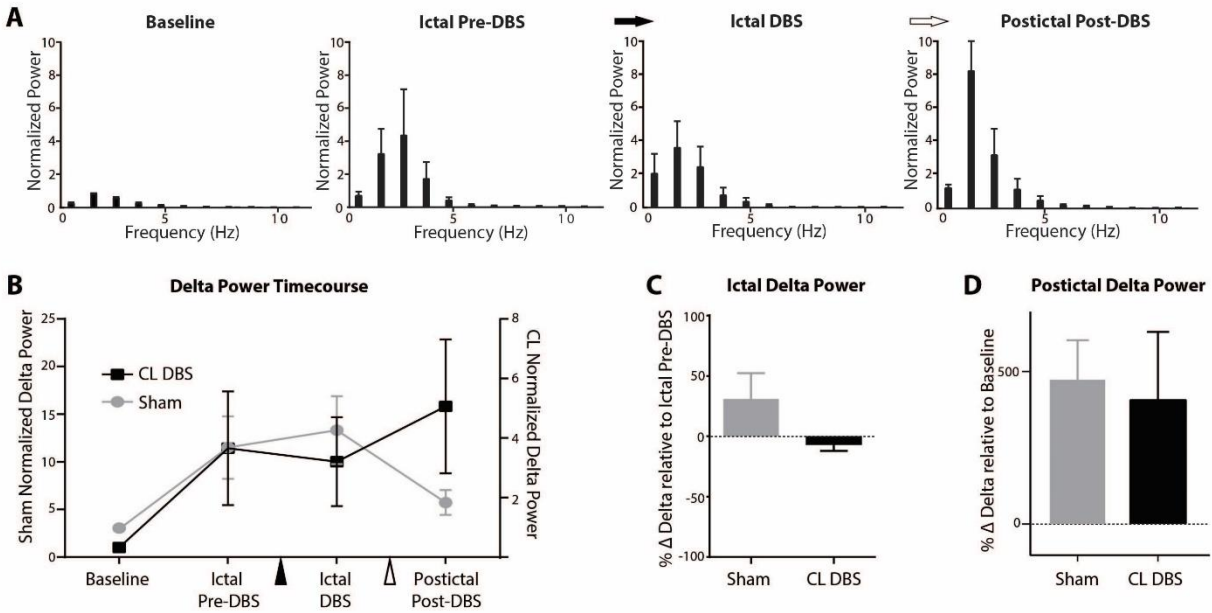
Supplementary Figure 2. Example of stimulation and group data for PnO stimulation in animals under deep anesthesia. (A) PnO DBS under deep anesthesia eliminates cortical slowing. **(B)** 10-second-long magnified insets of marked pre-DBS, intra-DBS, and post-DBS epochs exemplify desynchronized lateral orbital frontal cortical local field potential (Ctx LFP) with increased tonic firing in multi-unit activity (MUA) intra- and post-stimulus. **(C)** Group averaged data in 20 s epochs showing that PnO DBS decreases low-frequency power during and after stimulation. Black arrow indicates onset and white arrow end of PnO DBS. **(D)** Time course of delta-band (0 – 4 Hz) power before, during, and after stimulation. Pre-DBS and intra-DBS epochs are 20 s. Timecourse following DBS is shown with 10 s epochs. There is a significant difference between the DBS and sham conditions in all intra- and post-DBS epochs. Black arrowhead indicates onset and white arrowhead end of PnO DBS. **(E)** Change in delta power from pre-DBS baseline during stimulation (Stim) is significantly greater than sham controls (20 s epochs). $n = 7$ animals for C – E. Same animals as Figure 3 except for 2 animals that did not have stimulation under deep anesthesia. All results are mean \pm SEM. ** $p < 0.01$, *** $p < 0.001$, Bonferroni-Holm corrected.



Supplementary Figure 3. Cortical physiological arousal with PnO DBS in focal limbic seizures in awake animals. (A) PnO DBS during focal limbic seizure in an awake behaving animal decreases cortical slowing. Seizure was induced by 2 s, 60 Hz stimulation of hippocampus (HC). Break in recording of 90 s, during which seizure eventually ceases and DBS continues, enables display of the post-DBS time period. Total DBS duration was 120 s. **(B)** 3-second-long magnified insets of marked baseline, ictal pre-DBS, ictal DBS, postictal DBS, and postictal post-DBS epochs exemplify desynchronized lateral orbital frontal cortical local field potentials (Ctx LFP) with DBS. **(C)** PnO DBS decreases low-frequency power during ictal DBS, postictal DBS,

and postictal post-DBS epochs. Black arrow indicates onset and white arrow end of PnO DBS.

(D) Time course of delta-band (0 – 4 Hz) power during each epoch compared to sham stimulation. There is a significant difference between the DBS and sham conditions during the ictal DBS, postictal DBS, and postictal post-DBS epochs. Black arrowhead indicates onset and white arrowhead end of PnO DBS. **(E)** Ictal DBS delta-band power relative to the ictal pre-DBS delta power is significantly decreased compared to sham stimulation. **(F)** Postictal DBS and postictal post-DBS delta band power relative to baseline delta power remains elevated in the sham case and is returned to near-baseline levels in the simulation case. All results are mean \pm SEM. N=8 animals for C - F. * $p < 0.05$, Bonferroni-Holm corrected.



Supplementary Figure 4. CL stimulation alone does not produce physiological arousal during focal limbic seizures. Seizures were induced by 60 Hz, 2 s hippocampal stimulation under light anesthesia. CL DBS was performed 10 s after seizure onset using 20 s stimulus train duration. **(A)** CL DBS does not effectively decrease low-frequency power in lateral orbital frontal cortical local field potential recordings during ictal DBS or postictal post-DBS epochs. Black arrow indicates onset and white arrow end of CL DBS. **(B)** Time course of cortical delta-band (0 – 4 Hz) power during each epoch compared to sham stimulation. There were no significant differences between DBS and sham conditions during all epochs. Black arrowhead indicates onset and white arrowhead end of CL stimulation. **(C)** Ictal stimulus delta-band power relative to ictal pre-DBS delta-band power is not significantly decreased compared to sham stimulation. **(D)** Postictal post-DBS delta-band power relative to baseline delta-band power remains elevated in sham and DBS conditions. N= 3 animals. All results are mean \pm SEM.

Supplementary Video.**Dual-site CL + PnO deep brain stimulation restores normal exploratory behavior during focal****limbic seizure.** Prior to seizure induction both the sham control (left) and DBS (right) rats

exhibit normal exploratory movements in the cage. Following onset of focal limbic seizure

induced by 2s, 60 Hz hippocampal stimulation behavioral both animals exhibit behavioral

arrest. With initiation of dual-site CL + PnO DBS (100 Hz, 300 μ A, 120 s in CL; 50 Hz, 150 μ A, 120s in PnO for DBS animal on right; same parameters but 0.2 μ A stimuli for sham control on left)

the DBS animal (right) immediately resumes normal exploratory behaviors including forepaw

and hindpaw ambulation, sniffing/whisking and touching sides of the cage with forepaws, while

the sham control animal (left) remains frozen in position. Simultaneous EEG (LFP) recordings in

both animals exhibited hippocampal seizure activity throughout, accompanied by lateral orbital

frontal cortical 1-2 Hz slow wave activity which continued in the sham control animal but

transitioned to a normal awake-appearing desynchronized pattern in the DBS animal (not

shown, but similar to recordings in Fig. 5). At the end of the seizure both animals explore the

cage normally however the sham control (left) exhibits wet-dog-shakes and epileptiform

polyspike discharges (not shown) in the postictal period which are not present in the DBS

animal (right). Normal exploratory behaviors continue throughout the DBS period for the

animal on the right and no change in these behaviors occurs after DBS termination. Video may

downloaded at https://files.yale.edu/public_download?shareId=28e6d9f8ad2a013e1bd945f143bd7b14 until2/15/2016 or requested by emailing adam.kundishora@yale.edu.

Appendix A: Additional information on stimulus parameters

In the initial phases of experimentation, during which multiple arousal nuclei were being explored, a wide range of stimulation parameters were explored. This was secondary to the assumption that each nuclei, with its unique composition of interneurons, differently sized cell bodies, *en passant* fibers, and tonic firing rate might respond differently to the same set of stimulation parameters. The only parameters which were ubiquitously applied to all stimulations were the waveform, which was chosen to be a biphasic square wave, and the number of stimulation poles, which was chosen to be bipolar as opposed to unipolar. With regard to the waveform, biphasic square wave stimulation reflects the current norm of electrical stimulation in both experimental animal models and clinically in humans. Bipolar stimulation as opposed to unipolar stimulation was chosen because of our available stimulation equipment and background knowledge from previous experiments.

The parameters that were varied included: stimulation amplitude (amps), pulse width/phase width (s), frequency (Hz), and pattern (continuous vs. intermittent vs. interleaved) (Appendix Fig. 1 A, B). These parameters were systematically and independently varied in each nuclei while the animal was under deep anesthesia. The measure of efficacy was the presence of cortical desynchronization during the stimulation and the duration of persistent desynchronization following the stimulation. Once optimized, the parameters were then applied to ictal periods while the animal was under light anesthesia, as described in the methods section. All reported stimulation parameters throughout this paper represent the optimized set determined in the aforementioned fashion.

Appendix B: Additional information on other arousal nuclei

An initial exploratory phase was undertaken to identify known arousal nuclei that might be candidates for stimulation during seizure. The following represent nuclei which were stimulated and found to have a desynchronizing effect on the cortex while the animal was under deep anesthesia. Each nuclei was then tested during an ictal period, demonstrating varying efficacy at abolishing slow waves.

Cortical physiological arousal with central medial thalamic stimulation under deep anesthesia and during limbic seizure

The central medial thalamic nucleus (CM), like CL, is a member of the intralaminar thalamus which is known to have widespread cortical and subcortical projections to areas involved in arousal and attention (33, 61). Optimum stimulation parameters were determined to be: 200 – 400 μ A split bilaterally, 500 μ s phase width, at 100 Hz, continuously. An example of an interleaved stimulation is given to demonstrate the on-off effect of 100 Hz vs. 600 Hz stimulation (Appendix Fig. 2 A). During ictal periods, CM stimulation was insufficient at desynchronizing the cortex (Appendix Fig. 2 B). In total, 4 animals were tested with bilateral CM stimulation.

Cortical physiological arousal with ventromedial thalamic stimulation under deep anesthesia and during limbic seizure

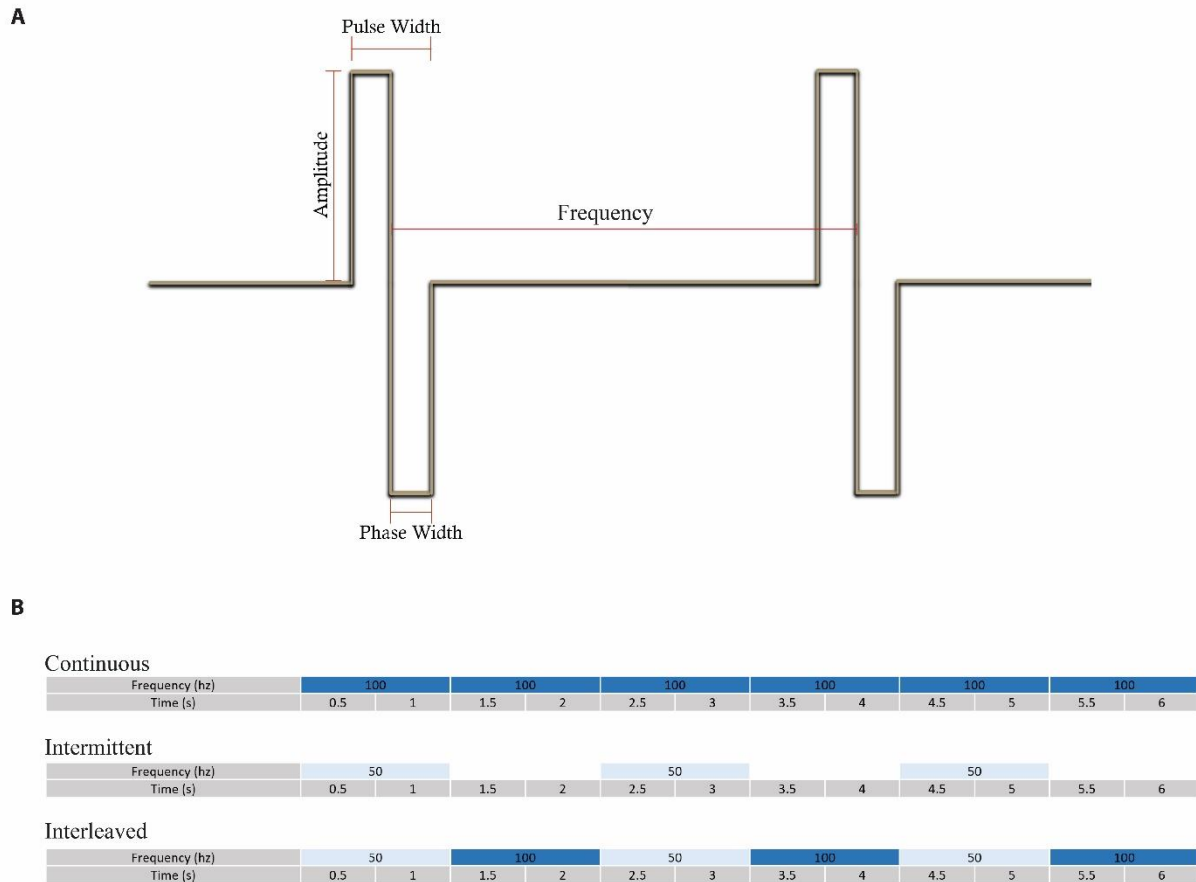
The ventromedial thalamic nucleus (Vm) is characterized by extremely wide spread neocortical projections. It lies deep to the intralaminar thalamus and is a place of convergence for many pathways, including the deep cerebellar nuclei, reticular thalamus, and the mesencephalic reticular formation. Optimum stimulation parameters were determined to be: 300 – 500 μ A split bilaterally, 500 μ s phase width, at 100 Hz, continuously. When stimulated under deep anesthesia, cortical desynchronization was robust. Like CL and CM, Vm also proved insufficient to desynchronize the cortex during seizure, under light anesthesia (see methods). However, unlike the other thalamic nuclei tested, stimulating Vm did sometimes have an effect late in the seizure evolution (Appendix Fig. 3 A, B). This effect was inconsistent across trials within the same animal, but was noted in more than one animal, perhaps implying that unknown variables about the seizure itself influence the efficacy of stimulation. It was this inconsistency that drew us away from choosing Vm as a partner to PnO in dual stimulation experiments. In total, 4 animals were tested with bilateral Vm stimulation.

Cortical physiological arousal with deep mesencephalic stimulation under deep anesthesia and during limbic seizure

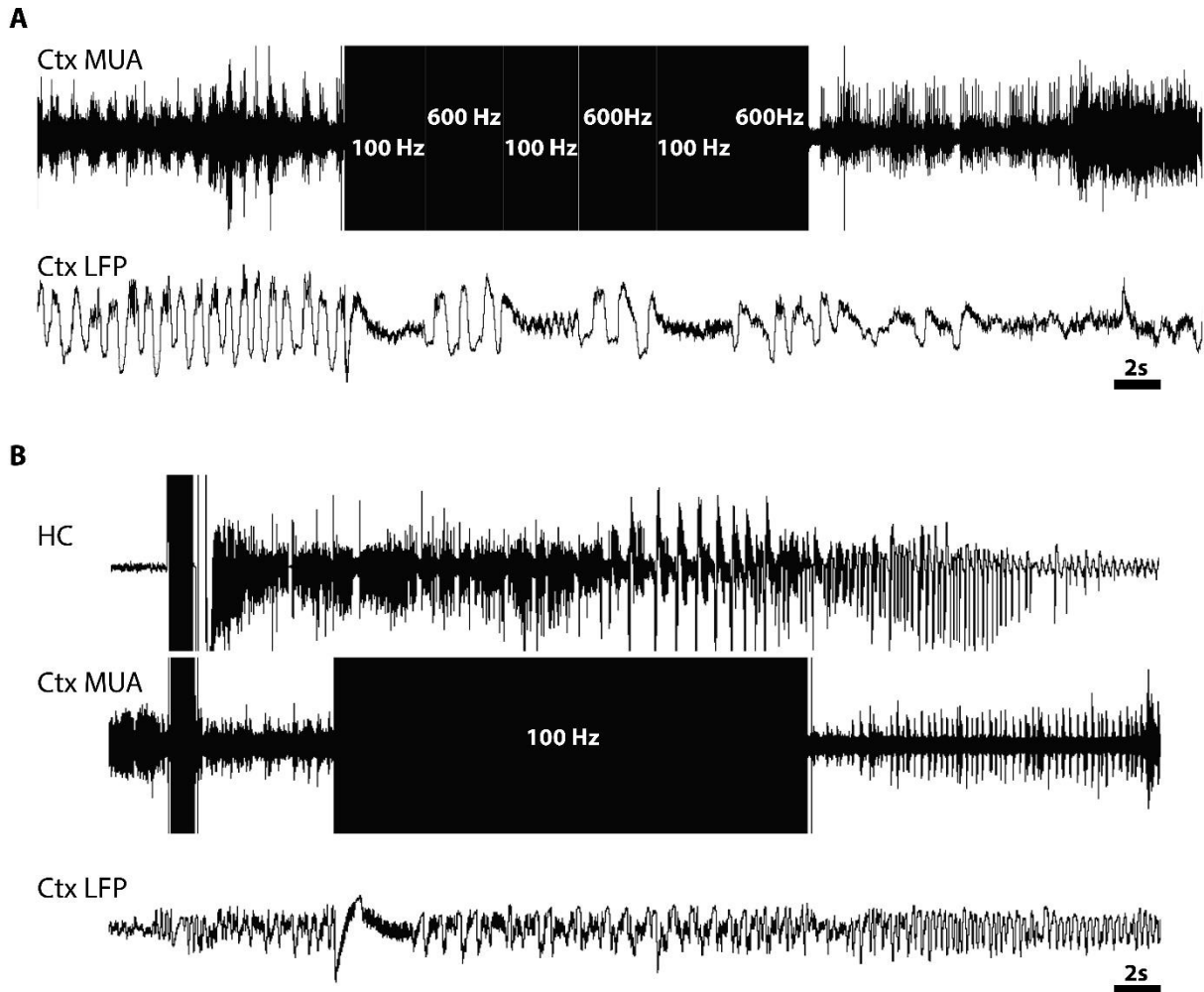
The deep mesencephalic nucleus (DpMe) describes a group of cells, dorsal to the PnO, extending rostrally into the midbrain, constituting part of the midbrain reticular formation (33). With rich projections to the thalamus and cortex, this brain area is known to play a role in sleep, arousal, and consciousness. Optimum stimulation parameters were determined to be:

30 – 100 μ A split bilaterally, 500 μ s phase width, at 50 Hz, continuously. DpMe stimulation under deep anesthesia, like PnO stimulation, was robustly effective (Appendix Fig. 4 A). Ictally, under light anesthesia, DpMe stimulation also showed promise at abolishing slow waves (Appendix Fig. 4 B). When directly compared to PnO stimulation, albeit with a low sample size, PnO proved to have a greater reduction of slow waves than DpMe stimulation. In our opinion however, DpMe remains a target to be explored further both in the lightly anesthetized ictal state and the awake ictal state. In total 4 animals were tested with bilateral DpMe stimulation.

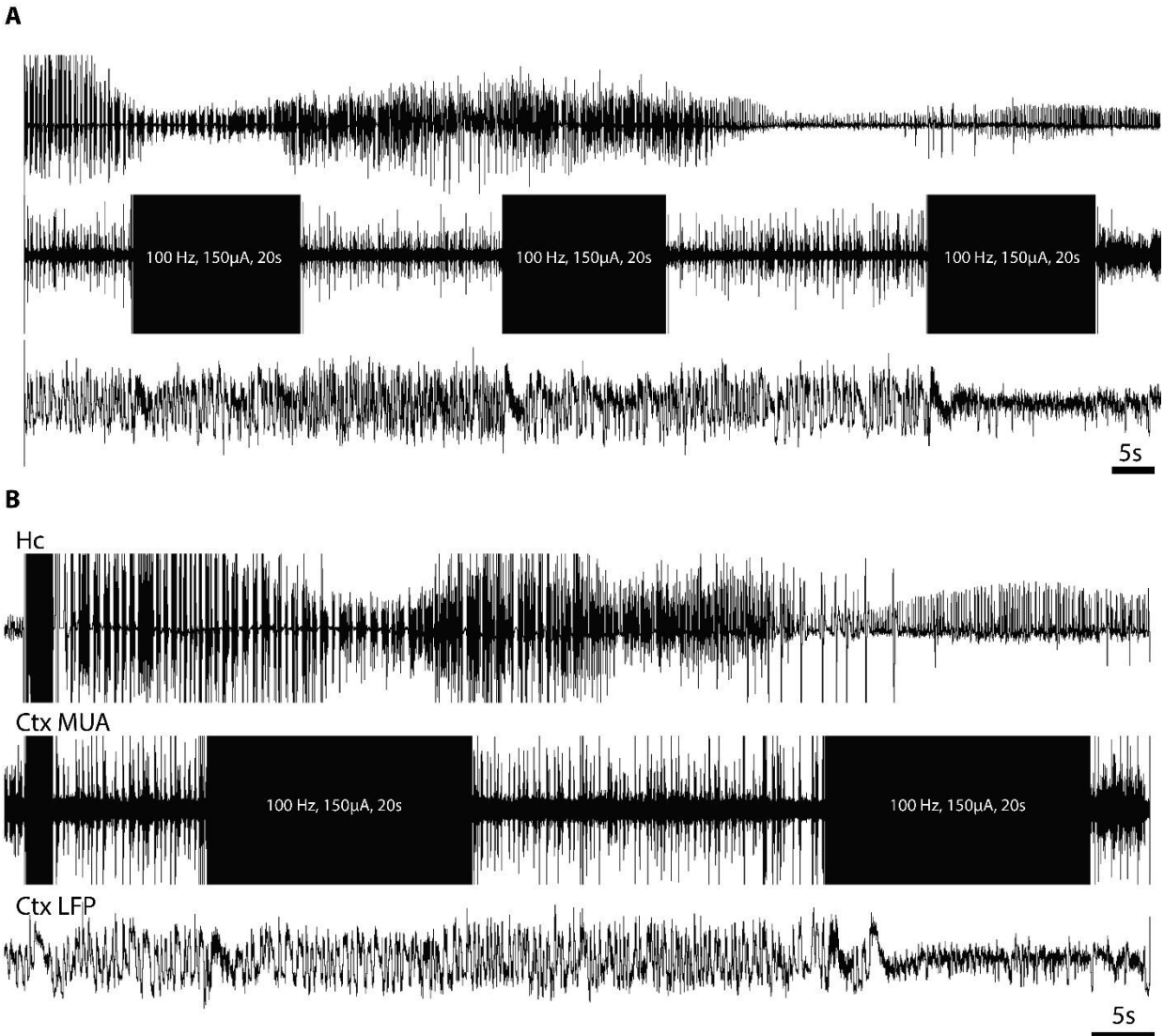
Appendix Figures



Appendix Figure 1. Stimulation parameters and pattern. (A) Diagram representing the 4 characteristics of a waveform that were varied during experimental determination of optimum stimulation parameters. **(B)** Schematic representation of the three types of stimulation patterns tested in each arousal nuclei.

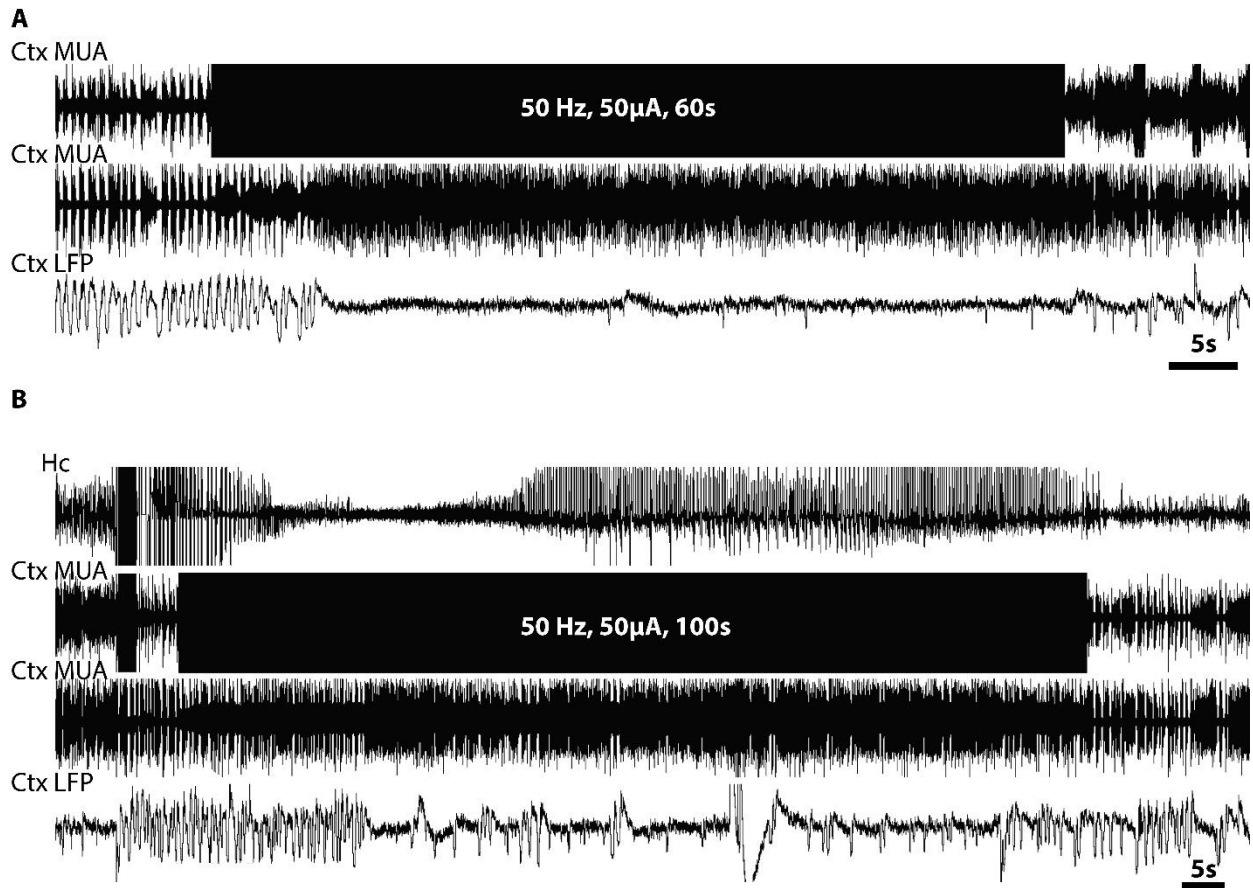


Appendix Figure 2. Stimulation in central medial thalamic nucleus. (A) Interleaved stimulation demonstrates as response (cortical desynchronization) to 100 Hz and no response to 600 Hz. **(B)** Stimulation continuously at 100 Hz during limbic seizure is insufficient to desynchronize the cortex. Ctx LFP: cortex local field potential; Ctx MUA: cortex multiunit activity; HC: hippocampus.



Appendix Figure 3. Stimulation in ventromedial thalamic nucleus. (A) Stimulation of Vm was ineffective at desynchronizing the cortex during approximately the first minute of the seizure, as is evidenced by persistent cortical slow waves through the first two stimulations. The third stimulation, occurring 1 minute and 45 seconds into the seizure does show effective desynchronization. At this point, the amplitude of the hippocampal discharges are significantly lower than at seizure onset. **(B)** A second example showing a similar pattern of ineffective

stimulation early in the seizure transitioning to effective stimulation late in the seizure. Ctx LFP: cortex local field potential; Ctx MUA: cortex multiunit activity; HC: hippocampus;



Appendix Figure 4. Stimulation in deep mesencephalic nucleus. (A) There is robust removal of slow waves and full cortical desynchronization during stimulation under deep anesthesia. **(B)** Stimulation during limbic seizure shows a partial desynchronization with occasional ‘break through’ slow waves.